ROLE OF XERODERMA PIGMENTOSUM COMPLEMENTATION GROUP B (XPB) IN GENOME MAINTENANCE UNDER OXIDATIVE STRESS

TING POH LEONG ALOYSIUS
(B.Sc.(Hons.), NUS)

A THESIS SUBMITTED

FOR THE DEGREE OF MASTER OF SCIENCE

DEPARTMENT OF PHYSIOLOGY

YONG LOO LIN SCHOOL OF MEDICINE

NATIONAL UNIVERSITY OF SINGAPORE
2008

ACKNOWLEDGEMENTS

This thesis would not have been possible without a number of people to whom I wish to extend my thanks. First and foremost, I would like to thank my supervisor, Associate Professor Manoor Prakash Hande for his guidance and support throughout my candidature. Thank you for the opportunity to work on an exciting and novel project which included the chance to attend two conferences.

I wish to extend my gratitude to members of my lab, the Genome Stability Lab, for the friendship and memories. Their instruction of me when I first joined the lab, assistance when I had difficulties in experimental procedures are only the tip of the iceberg. Special mention goes to Ms Low Kah Mun Grace who mentored me during my Honors year and who continued to be a source of inspiration during my Masters project and to Mr Khaw Aik Kia who as lab officer inculcated in me proper research etiquette and decorum.

A thank you also to members of other labs in the Department of Physiology who have helped me with advice on techniques and protocols, especially members of the Cancer Metastasis and Epigenetics Lab, ROS and Apoptosis Lab, Nuclear Receptors Lab and Hepato-Oncogenetics Lab.

TABLE OF CONTENTS

CHAPTER 3

CHAPTER 4

LIST OF FIGURES

SUMMARY

Introduction: Xeroderma Pigmentosum B (XPB/ ERCC3/ p89) is an ATP-dependent 3'→5' directed DNA helicase involved in basal RNA transcription and the nucleotide excision repair pathway (NER). While the role of NER in alleviating oxidative DNA damage has been acknowledged it remains poorly understood.

Aim: This study aims to investigate the role of XPB in cellular response to oxidative stress induced DNA damage.

Method: Primary fibroblasts derived from a patient suffering from XP/CS complex due to a mutation in XPB, a heterozygous parent and a normal individual were treated to with hydrogen peroxide (H_2O_2). Cellular response was measured with assays gauging cytotoxicity, genotoxocity, growth kinetics and mechanistic effect.

Results and Discussion: A deficiency in functional XPB paradoxically renders cells less sensitive to the cytotoxic effects of oxidative stress while increasing the genotoxic effects. XPB dysfunction also impedes damage response mechanisms. These effects are due to alterations in the cellular response to oxidative stress including important players such as p53 and telomeres.

Conclusion: These findings have implications in the mechanisms of DNA repair, mutagenesis and carcinogenesis and aging in normal physiological systems. Our study expands knowledge of the role of XPB in protection against oxidative assault.

CHAPTER 1

INTRODUCTION

INTRODUCTION

Xeroderma Pigmentosum B (XPB/ ERCC3/ p89) is an ATP-dependent 3'→5' directed DNA helicase involved in basal RNA transcription and the nucleotide excision repair pathway (NER). While the role of NER in alleviating oxidative DNA damage has been acknowledged it remains poorly understood. Oxidative damage to telomeres has been shown to accelerate telomere attrition, a phenomenon which has been correlated to aging and cancer. Other helicase domain containing proteins have been reported as facilitators of normal telomere function. It has also been reported that another component of the pathway, Xeroderma Pigmentosum F (XPF) is involved in telomere dynamics in mice.

To study the involvement of XPB in repair of oxidative DNA damage, we utilized primary fibroblasts from a patient suffering from Xeroderma Pigmentosum with Cockayne Syndrome and Hydrogen Peroxide (H_2O_2) to induce oxidative stress.

Mutant cells retained higher viability and presented cell cycle dysfunction after H_2O_2 exposure. Single cell gel electrophoresis (Comet) assay showed that the mutation caused a reduced repair capacity for oxidative DNA damage. Cytokinesis blocked micronucleus assay revealed increased genome instability induced by H_2O_2. Mutant fibroblasts were also displayed decreased population doubling rate, increased telomere attrition rate and early emergence of senescent characteristics under chronic low dose exposure to H_2O_2. Western blotting revealed XPB was upregulated in response to H_2O_2 exposure and mutant cells displayed aberrant regulation of p53. Fibroblasts from a heterozygous individual displayed intermediate traits in some assays and normal traits in others, indicating possible copy number dependence.

The results show that a deficiency in functional XPB paradoxically renders cells less sensitive to the cytotoxic effects of oxidative stress while increasing the genotoxic effects. These effects are due to profound alterations in the cellular response to oxidative stress when XPB is dysfunctional, including important players in genome stability such as p53 and telomeres.

These findings have implications in the mechanisms of DNA repair, mutagenesis and carcinogenesis and aging in normal physiological systems. Our study supports the already established importance of XPB in genome maintenance and expands its role to protection against oxidative assault. It also implicates oxidative stress as a possible major contributor to XP clinical presentations, particularly at tissues away from the body surface and hence protected from UV exposure.

1.1 Objectives:

This study aims to elucidate the role of XPB in cellular response to oxidative stress by focusing on the following aspects

- **The role of XPB on oxidative DNA damage repair competency and genomic stability**
- **The role of XPB on growth kinetics and telomere dynamics**
- **The role of XPB in oxidative stress response mechanisms**

CHAPTER 2

LITERATURE REVIEW

LITERATURE REVIEW

2.1 DNA damage and repair – links to aging and oncogenesis

Genomic assault as a result of exposure to both endogenous and exogenous genotoxic agents is a constant and invariable phenomenon. DNA damage is a highly detrimental consequence of such stress. This is because DNA is the material that carries critical information and directs all processes necessary for life. As such it is the only biological macromolecule that is repaired if damaged. Assault on DNA can threaten its intrinsic structure and composition. Such assaults can manifest as single or double DNA strand breaks, simple base deletions, insertions or point mutations, instability of hydrogen bonds between complementary strands and adducts between adjacent bases or with other molecules, all of which distort the DNA helix and alter important information coded, thereby interfering with DNA replication and protein transcription and predispose oncogenesis and other developmental defects (Hoeijmakers, 2001). DNA damage may also occur at telomeres, a process which can compromise their integrity. As telomeres are important factors in genome integrity and replication competency, damaged telomeres can lead to outcomes such as genomic instability and premature senescence (Gilley et al., 2005; Klapper et al., 2001; Levy et al., 1992; Rodier et al., 2005; Shay and Wright, 2001).

Organisms are thus equipped with mechanisms to circumvent these deleterious events. These include cell cycle arrest mechanisms that allow determination of the extent of DNA damage. In the event that the damage is too severe for effective repair, arrest proceeds to apoptosis Mammals have evolved to be equipped with DNA repair mechanisms that specifically operate for individual base damages as well as genome

repair through recognizing specific DNA helix distortions, one of which is the versatile nucleotide excision repair (NER) pathway (Wood, 1997).

2.2 Reactive Oxygen Species (ROS) in DNA damage

Reactive oxygen species (ROS) are known to cause oxidative damage to cellular components, as well as a multitude of DNA lesions (Finkel and Holbrook, 2000; Dizdaroglu, 1992). Hydrogen peroxide (H_2O_2) is an endogenously produced ROS, generated during oxidative energy metabolism and exposure to exogenous factors such as lead (Pb) compounds. Similar to UV-induced DNA damage, oxidative DNA damage gives rise to helix distortions that hinder base pairing, transcription and replication. Accumulation of unrepaired oxidative lesions predisposes cancer (Hoeijmakers, 2001) and shortens telomeres (von Zglinicki, 2002), leading to premature senescence and possibly aging. H_2O_2 presents a particular hazard as it can be converted to the more reactive hydroxyl radical (·OH) by the Fenton reaction. This reaction occurs in the nucleus (Halliwell and Gutteridge, 1992; Imlay et al., 1988) and thus can lead to DNA damage. It also produces Fe^{3+} ions which can yield more ·OH by the Haber-Weiss reaction between superoxide and hydrogen peroxide. The rate of endogenous ROS production is directly correlated to the metabolic activity of the cells. During physical exertion or upon exposure to exogenous agents such as sodium arsenite, high amounts of ROS are produced, and mechanisms for its removal might be overwhelmed. Buildup of oxidative lesions predisposes cancer (Hoeijmakers, 2001) and accelerates telomere attrition, leading to premature senescence and possibly aging (Harman, 1956; de Boer et al., 2002; von Zglinicki, 2002; Rybanska and Pirsel, 2003). In support of this theory, it has been shown that H_2O_2 exposure causes cultured cells to senesce prematurely (von Zglinicki, 2002), possibly due an accelerated rate of telomere attrition and DNA lesions

(Duan et al., 2005); while antioxidant enzymes and substances slow down telomere shortening rate (Serra et al., 2003; Kashino et al., 2003).

2.3 Nucleotide Excision Repair (NER) and Xeroderma Pigmentosum (XP)

Xeroderma Pigmentosum is a rare autosomal recessive congenital DNA repair disorder that results in segmental progeria. The cause is a defect in any of the 8 XP proteins (XPA through XPG and XP-V), which make up the 8 XP complementation groups. The most severe form of the disease is observed in individuals with defective XPA (Wood, 1997). XP patients suffer from sunlight hypersensitivity, developing severe sunburns with onset of poikilodermia on light-exposed skin. The inability to repair DNA lesions also predisposes patients to a 1000-fold increase in risk of cutaneous cancers, particularly squamous and basal cell carcinomas, and malignant melanomas from early childhood, resulting in high mortality rates before adulthood (van Steeg and Kraemer, 1999; Norgauer et al., 2003). Other symptoms include neurological and developmental abnormalities, blindness, loss of hearing and sparse hair. Patients also present with brittle skin and hair defects due to transcriptional interference by DNA lesions. Defects in the NER can also cause Cockayne's syndrome (CS) and trichothiodystrophy (TTD) (Hoeijmakers, 2001; van Steeg and Kraemer, 1999; Norgauer et al., 2003).

The NER pathway is conserved among lower and higher eukaryotes. It is a highly versatile system that involves the excision of single stranded oligonucleotides containing bulky DNA lesions that would interfere with normal cellular process. In humans, the NER pathway is known to facilitate the removal of UV-induced pyrimidine dimers and lesions caused by cigarette smoke (Sancar, 1996). This highly organized mechanism engages a multiplex of proteins in a temporally specific manner. Two sub-pathways exist, namely global genome repair (GPR) and transcription coupled repair (TCR), which differ in their coverage and at the initial damage detection step. GGR directs genome-wide

excision of lesions from non-transcribed regions to non-transcribed strands of transcribed regions while TCR controls removal of DNA lesions in transcribed regions which hinder transcription elongation by RNA polymerase II.

Initiation of the pathway involves identification of the site of damage and unwinding of the proximal DNA double helix. Subsequently, excision of a ~24-32 base pair long oligonucleotide containing the damage occurs. Repair concludes with synthesis to replace the excised strand and ligation by standard DNA polymerases and ligases, restoring the native state of the DNA (Hoeijmakers, 2001; Wood, 1997). The entire reaction requires at least 27 proteins including the 8 xeroderma pigmentosum (XPA-G and XP-V) proteins, the trimeric replication protein A [RPA, human single-stranded DNA binding protein (HSSB)], and the multisubunit Transcription Factor II F (TFIIF) (Sancar, 1996; Wood, 1997; Hoeijmakers, 2001) in a specific and temporal manner.

Although the symptoms of XP have been traditionally ascribed to UV-induced damage, it is difficult for such assaults to account for the totality of XP symptoms, particularly in organ systems not directly exposed to sunlight. Repair of oxidative lesions is largely carried out by the base excision repair (BER) pathway. However, several NER factors appear to modulate BER by interacting with and stimulating DNA glycosylases which initiate the BER (Sugasawa, 2008). One type of oxidative lesions, 8,5'-cyclopurine-2'-deoxynucleosides, is specifically repaired by NER and may play a role in the occurrence of cancer and neurodegeneration seen in XP patients (Brooks et al., 2000; Kuraoka et al., 2000). Oxidative base lesions have also been implicated in patients suffering from the XP/CS complex, who display the skin and eye diseases of XP and the somatic and neurological abnormalities of CS (Lindenbaum et al., 2001; Oh et al., 2007;

Oh et al., 2006; Rapin et al., 2000). ROS generation and subsequent oxidative stress has also been shown to occur downstream of various other genotoxic agents including UV (Finkel and Holbrook, 2000). Furthermore, the neurological symptoms of XP/CS may be caused by faulty DNA repair to neuronal cells induced by oxidative metabolism or other endogenous processes (Kraemer et al., 2007). The NER protein Cockayne Syndrom, Type B (CSB) was also found to have a role in transcriptional response following oxidative stress. Cells defective in CSB showed down-regulation of several proteins related to stress response, transcription, translation, signal transduction and cell cycle progression following exposure to H_2O_2 induced oxidative stress; failure to induce expression of ribosomal proteins was also observed (Kyng et al., 2003). It is therefore hypothesized that oxidative stress may thus be an important player in the development of XP. We have previously found evidence in support of this in cells from patients with XP resulting from Xeroderma Pigmentosum A (XPA) deficiency (Low et al., 2008). XPA deficient cells were interestingly resistant to the cell death induced by H_2O_2 but had increased hallmarks of genomic instability.

2.4 XPB – current knowledge, future discoveries

XPB is a 3'→5' helicase in the NER pathway and a subunit of the RNA polymerase II holoenzyme TFIIH. XPB plays a key role in the NER by unwinding the DNA helix surrounding the lesion and thus allowing access by subsequent factors. Studies have also shown roles for XPB in the demarcation and verification of damage(Sugasawa, 2008), incision (Coin et al., 2004) and excision (Wakasugi and Sancar, 1998) of lesions and in the recruitment of other NER factors to lesion sites (Oh et al., 2007). As a subunit of TFIIH, XPB plays a role in basal transcription (Akoulitchev et al., 1995). As such, XPB mutation can give rise to all three NER dysfunction syndromes (Lehmann, 1995). XPB is a member of the helicase domain containing family of proteins. Other members of this family including WRN and BLM has been shown to have a role in telomere maintenance (Lee et al., 2005; Du et al., 2004; Opresko et al., 2005; Bai and Murnane, 2003; Crabbe et al., 2004). Additionally, it has been reported that another NER factor, the endonuclease XPF is involved in telomere shortening in mice overexpressing Telomere Repeat Binding Factor 2 (TRF2) (Munoz et al., 2005). XPB also has other roles outside of the NER and DNA repair. It appears to function in epigenetic control through the DNA demethylation induced by Gadd45a overexpression. XPB has also been demonstrated to bind to p53 and have a partial-redundant role in p53 mediated apoptotic signaling. Although the NER has been shown to play a role in oxidative damage repair, no specific study has been done to investigate the importance of specific members. The multiple implications of XPB thus make it an interesting candidate for the study of the NER pathway in resolving oxidative DNA damage.

2.5 DNA repair factors and telomeres – a close knit relationship

Various studies have shown an increasingly close link between telomere regulation and DNA repair (d'Adda et al., 1999; d'Adda et al., 2001; Gilley et al., 2001; Hande et al., 2001; Hande, 2004; Hande et al., 1999b; Hsu et al., 2000; McPherson et al., 2006; Slijepcevic et al., 1997). Telomeres are non-coding DNA sequences (TTAGGG in humans), associated with a number of proteins, that cap the ends of chromosomes and are thought to serve two functions (Rodier et al., 2005). Firstly, they are believed to protect chromosomes from break-fusion-break bridges, thereby preventing chromosome aberrations that result in deregulation of pathways that regulate cell proliferation and thus predispose cancer. To counter this, cells in which telomere attrition has reached a critical limit become senescent to prevent further shortening. This is effectively a cellular clock, the second function of telomeres, which has been proposed as a determinant in aging and lifespan. Interestingly, telomere attrition has been shown to be accelerated by factors such as oxidative stress and ultraviolet radiation. Cultured human fibroblasts have been shown under senescence prematurely when exposed to such conditions (Tchirkov and Lansdorp, 2003). Duan *et al* (2005) suggested that this stress-induced premature senescence (SIPS) involves genes related to DNA-damage-and-repair and telomere shortening and shares the same mechanisms with replicative senescence *in vivo*.

ATM, a general DNA damage repair protein, has been implicated in the repair of telomeric DNA via nucleotide excision repair pathways, whereby ATM deficiency led to accelerated telomere shortening (Tchirkov and Lansdorp, 2003; Hande et al., 2001) and extrachromosomal telomere fragments. The Werner syndrome helicase, WRN, has been found to be involved in telomere repair post-oxidative stress (Lee et al., 2005). Werner

syndrome shares many outward symptoms with XP, including premature aging and skin defects. It is thus plausible that the helicases of the NER pathway might have a similar role to WRN. Lending further weight to the telomere-DNA repair factor link are recent findings regarding TRF2. TRF2 is a regulator of telomere length and binds the double stranded telomeric sequence specifically; it is essential for the formation and maintenance of t-loop structures *in vitro*. More over it was shown that TRF2 localises to double-stranded DNA breaks faster than the damage sensing protein, ATM, suggesting that telomere-binding factors such as TRF2 may be ancient and general DNA repair factors that have been exploited by the cell to protect telomeres (Stansel et al., 2001; Bradshaw et al., 2005).

2.6 Motivation and direction

We sought to study the effects of oxidative damage induced by hydrogen peroxide in cells derived from patients deficient in the XPB gene. The hitherto poorly defined role of the NER and its helicase XPB in oxidative DNA lesion repair and telomere dynamics in contrast to known roles for other DNA repair proteins such as ATM and WRN led us to investigate the possible role of the XPB in genome stability and telomere dynamics under oxidative stress.

Our study utilizes primary fibroblasts from individuals heterozygous for dysfunctional XPB as a result of a missense mutation (p.F99S) with the second allele being either dysfunctional as well due to a splice donor mutation in intron 3 (c.471+1G>A) or normal (henceforth designated $XPB^{-/-}$ and $XPB^{+/-}$ respectively) and Normal primary fibroblasts. The investigation employed crystal violet assay and cell cycle analysis to determine the effects of oxidative stress on cell viability and DNA damage checkpoint response. Cytokinesis-blocked micronucleus assay (CBMN) and metaphase analysis were used to study changes in genome stability. Single cell gel electrophoresis was performed to investigate repair proficiency. Subsequently, a cell kinetics study was carried out to determine the effects of chronic low dose oxidative stress. This study comprised telomere restriction fragment length analysis, population doubling studies. Finally, Western blots performed on cell cycle proteins were performed to gauge the efficiency of response to oxidative stress in XPB deficient cells. Our results show that XPB is involved in oxidative stress response. Deficiency in functional XPB paradoxically renders cells more sensitive to the genotoxic effects of oxidative stress while reducing cytotoxic effects, with modification in telomere dynamics. These findings

support the hypotheses that XPB is involved in the extrication of oxidative DNA damage and has a role in telomere dynamics under oxidative stress.

CHAPTER 3

MATERIALS AND METHODS

MATERIALS AND METHODS

3.1 Cell culture and H_2O_2 treatment

Primary human diploid fibroblasts from a normal individual (Normal GM03651E), an individual suffering from Xeroderma Pigmentosum complementation group B ($XPB^{-/-}$ GM13026) and the unaffected mother of the XPB patient ($XPB^{+/-}$ GM13027) were purchased from *NIGMS Human Genetic Cell Repository, U.S.A.,* and cultured in Minimal Essential Medium (MEM; *Gibco, U.S.A.*) supplemented with 15% fetal bovine serum (FBS; *Hyclone, U.S.A.*), 100U/mL penicillin/streptomycin, 1% vitamins, and 2% essential and 1% non essential amino acid. All cells were grown in a humidified 5% CO_2 incubator at 37^{o}C and maintained in a log phase. All other supplements unless otherwise stated were from *Gibco*. Exponentially growing cells were exposed to 20 μM, 40 μM, 60 μM, 80 μM and 100 μM of Hydrogen Peroxide (H_2O_2; *Kanto Chemical Co. Inc., Japan*) for 2 hours, following which the medium was replaced with fresh medium for a 22 hour recovery period.

For immunofluorescence and immunofluorescence-peptide nucleic acid fluorescence in situ hybridization (IF-FISH), HeLa cells were grown in supplemented MEM and seeded a density of 2 x 10^4 in Lab-Tek 2-well chamber slides (*Nunc, U.S.A.*) and treated with H_2O_2 for 30 minutes.

For co-immunoprecipitation, lymphoblastoids derived from a normal individual (GM03714A) were cultured in Roswell Park Memorial Institute (RPMI) 1640 medium (*Gibco Invitrogen Corporation, U.S.A.*) supplemented with 15% FBS and 1% L-Glutamine, were seeded at a density of 4 x 10^5 in 6 well plates (*Nunc, U.S.A.*) and treated with H_2O_2 for 2 hours.

3.2 Functional Studies

3.2.1 Crystal Violet Assay

Following treatment, cells were washed gently in 1 × PBS (*NUMI supplies*). Crystal Violet solution (0.75% crystal violet in 50% ethanol: distilled water with 1.75% formaldehyde and 0.25% NaCl) was gently added to the wells and incubated at room temperature, then washed in 1 × PBS. Thereafter, the wells were air-dried. A solution 1% dodium dodecyl sulphate (*SDS; NUMI supplies*) in 1 × PBS was added to lyse the cells and solubilize the dye. Solution absorbance at 595 nm was measured in an ELISA plate reader.

3.2.2 Cell Cycle Analysis by Fluorescence Activated Cell Sorting

Cells were fixed in 3:1 70% ethanol: 1 × PBS, and subsequently stained with propidium iodide (PI, *Sigma*): RNase A (*Roche, U.S.A.)* solution (2mg PI and 2mg RNaseA/100 mL 0.1% BSA in 1 × PBS). Samples were analysed by flow cytometry at 488nm excitation λ and 610 nm emission λ. A total of 10, 000 events were collected and the data obtained was analysed using WINMDI software.

3.2.3 Alkaline single cell gel electrophoresis (Comet) assay

Cells were harvested at two time points – immediately after 2 hour exposure to H_2O_2 and following the 22 hour recovery period. Harvested cells were resuspended in Hank's balanced salt solution (*HBSS; Sigma*), mixed with 0.7% low melting point agarose (*Conda, Spain*) and applied on Comet slides (*Trevigen, U.S.A.*). Embedded cells were subjected to lysis (2.5M NaCl, 0.1M EDTA pH 8.0, 10mM Tris base, 1% Triton X-

100) at 4˚C for 1 hour. After lysis, the slides were loaded onto a gel electrophoresis tank and immersed in alkaline electrophoresis buffer (0.3M NaOH buffered at pH 13 – 13.8 with 0.5M EDTA pH 8.0) for 40 minutes to allow DNA denaturation before being run at constant 25V/300 mA for 20 minutes. Following run, samples were neutralized with 0.5M Tris-HCl pH 7.5 (*NUMI supplies*) for 15 minutes, dehydrated in 70% ethanol for 5 minutes, then dried at 37˚C. DNA was stained using SYBR Green (*Trevigen*). Analysis of comets was performed using Comet Imager Software (*Metasystems, Germany*). Extent of DNA damage was expressed as a measure of comet tail moments. One hundred randomly selected cells were examined per sample.

3.2.4 Cytokinesis Blocked Micronucleus (CBMN) analysis

After 2 hour exposure, cells were incubated in fresh medium with 4.0 μg/mL cytochalsin B (*Sigma*) for 22 hours. Cells were subjected to hypotonic swelling in cold 0.075M potassium chloride (KCl), fixed using a combination of 3:1 methanol: acetic acid (Carnoy's) fixative and 6-7 drops of formaldehyde (to fix cytoplasm) and stored at 4^{o}C. Aged cells were dragged on a clean, dry slide, and the cytoplasm and nucleus were differentially stained with 30 μg/mL acridine orange. Nucleic material is stained yellow-green while cytoplasm is stained orange. One thousand binucleated cells with/without micronuclei were scored under the Axioplan 2 imaging fluorescent microscope (*Carl Zeiss, Germany*) with the appropriate triple band filter.

3.3 Cellular kinetic studies

3.3.1 Treatment

Cells were seeded in T75 flasks (*NUNC, U.S.A.*) at a density of 2 x 10^5 cells per flask and subjected to a 30 day long term, low dose chronic treatment. One set of cells was treated with 20μM H_2O_2 every 48 hours, with media changed prior to addition of drug; another set of cells was maintained in a Binder C150 incubator set at 40% volume O_2 (*Binder, Germany*), with media changed every 48 hours; media for control cells was also changed every 48 hours.

3.3.2 Morphological analysis

Cells were observed under a light microscope at 40×, 100× and 200× magnifications before media changes. Morphology of the cells was photographed using an Olympus C-7070 WZ digital camera (*Olympus, Japan*).

3.3.3 Population doubling (PD) study

Cells were harvested whenever 90% confluency was reached for untreated cells of each cell type, and on the final day of the experiment. This occurred on days 6, 12, 18, and 30. Harvested cells were counted using a hemacytometer. A fresh tissue culture flask was then reseeded with 2 × 10^5 cells, or all cells if cell numbers were less than 2 × 10^5.

The population doubling number (PDN) was calculated as follows:

$$PDN = \log_2(N_0/N_x),$$

where N_0 = number of cells at harvest and N_x= number of cells seeded (Greenwood et al., 2004)

A portion of the remaining cells was seeded in 6-well culture plates (*NUNC, U.S.A.*) for senescence-associated β-galactosidase (SA-β-gal) assay and the rest kept for DNA extraction for Telomere Restriction Fragment (TRF) analysis.

3.3.4 Senescence-associated β-Galactosidase (SA-β-gal) assay

Expression of SA-β-gal was performed using the Senescence β-Galactosidase Staining Kit (*Cell Signaling Technology, U.S.A.*) following manufacturer's instructions. Cells were observed under a light microscope at 40×, 100× and 200× magnifications, and cell photographs taken with an Olympus C-7070 WZ digital camera.

3.3.5 Telomere Restriction Fragment (TRF) length analysis

3.3.5.1 DNA extraction

Treated cells were harvested by trypsinsation. Total DNA was extracted using DNeasy Tissue Kit (*Qiagen*) at room temperature. Pelleted cells were resuspended in 200 µL 1 × PBS. Thereafter, 200 µL AL Buffer, and 20 µL Proteinase K was added to lyse the cells and remove proteins. The mixture was vortexed and incubated at 70 ˚C for 10 minutes, followed by the addition of 200 µ1 of ethanol. The mixture was vortexed and applied to DNeasy Mini Spin Column for adsorption of DNA to the column membrane. Washes with AW1 and AW2 were then carried out before eluting with AE buffer.

3.3.5.2 Telomere Length Measurement

The telomere lengths of were measured using TeloTAGGG Telomere Length Assay Kit (*Roche Applied Science, U.S.A*). Two micrograms of purified DNA was digested with *HinfI* and *RsaI* for two hours at 37°C. DNA fragments were separated by gel electrophoresis in 0.8% agarose gel at 60V for 3 hours, transferred via over-night Southern blot onto a nylon membrane and cross-linked onto the membrane using a UV cross-linker (Stratagene). Telomere restriction fragments were hybridized with telomere-specific digoxigenin (DIG)-labelled probe and incubated with Anti-DIG alkaline phosphatase and tetramethylbenzidine (TMB) according to manufacturer's protocol. Chemiluminescence signal was detected using X-ray film and telomere length was analysed using Kodak Molecular Imaging Software (*Kodak, U.S.A.*). Decrease in telomere length was then expressed as a function of PDN to assess the rate of telomere shortening, indicating the effect of drug treatment on telomeres.

3.4 Mechanistic Studies

3.4.1 Western Blotting

Cells were seeded, as described above and harvested at 2, 24 and 48 hours after exposure to H_2O_2. Total cellular protein was extracted by lysing cells in 100-200 µL lysis buffer (10 mM Tris-HCl (pH 7.4), 1% Sodium Dodecyl Sulfate (SDS), 1 mM sodium ortho-vanadate in ddH_2O). Released DNA was sheared by passing the lysate through a 0.4 x 12 mm syringe (*100 Sterican, BRAUN*). Lysed cells were centrifuged at 13.2 rpm, for 6 minutes at 4^oC, and the supernatants collected. Protein concentrations were determined using the micro BCA Protein Assay kit (*Pierce, USA*). One microlitre of cell

lysate was diluted in 249 µL of dH_2O and 250 µL micro BCA working reagent (25 parts solution A: 24 parts solution B: 1 part solution C) and quantified against known concentrations of BSA (1 µg/mL – 40 µg/mL). Forty micrograms protein from each sample was loaded into and run on 7.5% and 10% SDS-Polyacrylamide gel and then electro-blotted onto a nitrocellulose membrane (*BioRad Co., USA*). Transfer of proteins was checked by Ponceau Reagent (0.5 % Ponceau S *(Sigma, USA),* 1 % glacial acetic acid *(Sigma, USA)* in dH_2O). Membranes were blocked for 60 minutes with 5% non-fat milk in TBS-T (0.1% Tween-20 (*Sigma Aldrich, U.S.A.*) in 1 X TBS (0.1 M NaCl, 0.1 M Tris pH 7.4 in ddH_2O) (All purchased from *Numi, National University of Singapore*)) or 5% Bovine Serum Albumin (BSA, *Amresco, USA*) in 1 x TBS-T, depending on the protein probed for. Subsequently, membranes were probed with primary antibodies against target proteins overnight at 4˚C. Mouse monoclonal antibodies used were phosphorylated p53 (Ser 15) (p-p53) (*Cell Signaling, U.S.A*; 1:1000), p53 DO-1 (*Santa Cruz, U.S.A.*; 1:500), p21 F-5 (*Santa Cruz, U.S.A.*; 1:500) and actin (*Chemicon, USA*; 1:5000). Rabbit polyclonal antibody used was XPB (*Santa Cruz, U.S.A.*; 1:100). The membrane was then incubated in goat anti-mouse IgG (H+L)-HRP (*Pierce, USA*; 1:5000) or sheep anti-rabbit IgG (H+L)-HRP (*Pierce, USA*; 1:5000) secondary antibody for 1 hour at room temperature. The protein bands were visualized after incubation of membranes in Chemiluminescence Reagent Plus (*Perkin Elmer Life Science Inc, USA*) followed by exposure to X-ray film (*Pierce, U.S.A.*).

3.4.2 Immunofluorescence

Following H_2O_2 treatment, cells were washed in 1 × PBS and fixed in 4% paraformaldehyde (*Fisher Scientific, U.S.A*) for 10 minutes. After fixation, cells were immediately permeabilized with washing solution (0.2% Tween-20 in 1 × PBS) for 5 minutes and blocked with blocking solution (5% BSA in washing solution) for 30 minutes. 20 μL of primary antibody diluted in blocking solution was applied on cut pieces of parafilm (*Pechiney Plastic Packaging, Menasha, WI*). The slide with fixed cells was placed onto the parafilm pieces in upside-down orientation and turned up after checking to remove air bubbles. Slides were then incubated in a humidified chamber for 1 hour, following which they were washed with washing solution 3 x 5 minutes in a coplin jar. Parafilms were removed during the first wash. Secondary antibody diluted in blocking solution was applied as per the primary antibody and incubated in a humidified chamber at 37^{o}C for 1 hour, and washed as previously described. Slides were then fixed in 4% paraformaldehyde for 10 minutes and then washed with 1 x PBS (3 X 5 minutes) in a coplin jar. Slides were dehydrated in an ethanol series (70%, 90%, 100%), for 5 minutes each and air dried. Primary antibodies used were rabbit polyclonal XPB (*Santa Cruz, U.S.A.*; 1:100) and mouse monoclonal TRF2 (*Upstate, U.S.A.*; 1:200). Secondary antibodies used were Texas Red-labeled goat anti-mouse IgG (H+L) (*Invitrogen, U.S.A.*; 1:250) and Fluorescein-labeled goat anti-rabbit IgG (H+L) (*Vector Laboratories, U.S.A.*; 1:250). Slides were counterstained with Vectashield mounting medium containing DAPI (*Vector Laboratories, U.S.A.*) and stored in a light protected storage subsequent to visualization under an Axioplan 2 imaging fluorescence microscope (*Carl Zeiss, Germany*).

3.4.3 Immunofluorescence - Peptide Nucleic Acid Fluorescence In Situ Hybridization NA-FISH (IF-FISH)

Cells were labeled for XPB alone according to the previous steps. After completion of immunofluorescence, Cy3-labeled PNA-telomeric probe (*Applied Biosystems, U.S.A.*) was applied on to post-fixed slides as previously described (Hande et al., 1999a). Thermal co-denaturation was carried out at 80^{o}C for 3 minutes, following which slides were hybridized with in a humidified chamber at room temperature for 2 hours. Coverslip was removed carefully in wash solution 1 (70% formamide (*Merck, Germany*), 0.1% BSA, 0.01M Tris pH 7.4), and slides were washed in wash solution 1 for 2 X 15 minutes. Slides were then washed in wash solution 2 for 3 X 5 minutes. An ethanol series was then used to dehydrate slides, for 5 minutes each, after which they were air dried. Slides were counterstained with Vectashield mounting medium containing DAPI (*Vector Laboratories, U.S.A.*) and stored in a light protected storage subsequent to visualization under an Axioplan 2 imaging fluorescence microscope (*Carl Zeiss, Germany*).

3.4.4 Co-Immunoprecipitation (Co-IP)

3.4.4.1 Protein Extraction

Cells were seeded, treated with H_2O_2 and harvested as described previously, following which protein extraction was carried out. Cells were lysed in non-denaturing lysis buffer (50 mM Tris-HCl pH 8.0, 5 mM EDTA pH 8.0, 150 nM NaCl, 0.5% NP40, 1 mM PMSF, 1 mM sodium orthovanadate, ½ tablet of Roche Complete Mini (*Roche, U.S.A*)/ 5 mL lysis buffer). Cells were then pelleted at 1200 rpm, 5 minutes, 4^{o}C and

resuspended in cold 1 × PBS. This step was repeated before 300 µL cold non-denaturing lysis buffer was added. Cell suspension was passed through the a 0.4 x 12 mm needle several times, following which it was tumble-mixed end over end for 45 minutes. The suspension was then spun at maximum rpm for 30 minutes at 4^{o}C. Protein quantification was carried out using the Bradford Assay. 3 µL of cell lysate was diluted in 97 µL of dH_2O and 1 mL of GelCode protein staining reagent and quantified against BSA standards of known concentrations. A total of 1 mg of protein was used for immunoprecipitation and 50 µg of protein was used for Western Blotting to check total protein content.

Lysate containing 1 mg of protein was made up to 500 µL. The lysate was then pre-cleared by combining with 15 µL protein A-agarose beads and tumbled end over end for 30 minutes at 4^{o}C. Samples were thereafter microcentrifuged at 1000 rpm for 5 minutes at 4°C.

3.4.4.2 Antibody-beads conjugation

30 µL of protein A-agarose beads (*Invitrogen, U.S.A.*) or protein G-sepharose beads (*Zymed, U.S.A.*) were combined with 500 µL ice-cold 1 × PBS and 4 µg of antibody. Suspension was mixed thoroughly and tumble-mixed end over end for ≥ 1 hour at 4°C. Antibody-conjugated beads were then microcentrifuged at 1000 rpm for 2 minutes at 4°C. Supernatant was aspirated and 1 mL ice-cold non-denaturing lysis buffer was added following which tubes were inverted several times and another wash was carried out. Antibodies used were rabbit polyclonal XPB (*Santa Cruz, U.S.A.*; 4 µg),

mouse monoclonal p53 DO-1 (*Santa Cruz, U.S.A.*; 4 μg) and mouse monoclonal phosphorylated p53 (Ser 15) (*Cell Signaling, U.S.A*; 1:1000).

3.4.4.3 Immunoprecipitation

10 μL of 10% BSA was added to tubes containing antibody-bead conjugates. The entire volume of cleared lysate was then added and the mixture tumble mixed end over end for 4 hours at 4^{o}C. Samples were then microcentrifuged at 1000 rpm for 5 minutes at 4^{o}C. Supernatant was aspirated and 1 mL ice cold wash buffer (50 mM Tris-HCl pH 7.4, 150 nM NaCl, 5 mM EDTA pH 8.0, 0.1% Triton X-100) was added and the beads resuspended by inverting tube 3-4 times. Samples were microcentrifuged at 1000 rpm for 2 minutes at 4^{o}C. Supernatant was then aspirated, leaving ~ 20 μL. Wash steps were repeated 3 more times. Beads were washed once with 1 mL ice-cold 1 × PBS and aspirated completely using an extra fine glass pipette, leaving product of ~ 10 μL. 7 μL of 2 × Sample Buffer w/SDS and β-Mercaptoethanol (*Merck, Germany*) was added and samples boiled for 5-10 minutes. Western blotting was carried out to check for co-immunoprecipitation of XPB and p53.

3.5 Statistical Analysis

Statistical significance between and among data sets was assessed using two-way ANOVA, using Graphpad Prism. The difference was considered to be statistically significant when $^{*}P < 0.05$; **P<0.01; and ***P<0.001.

CHAPTER 4

RESULTS

RESULTS

4.1 Dysfunctional XPB desensitizes cells to the cytotoxic effects of oxidative stress

All three cell types exhibited a common trend of dose dependant decrease in cell viability (Fig. 1). Normal cells appeared to be more sensitive to H_2O_2 induced stress with significantly lower viability compared to the other two cells types from concentrations of 40 μM and above ($P<0.05$). $XPB^{-/-}$ cells appeared to be the least sensitive cell type with $XPB^{+/-}$ exhibiting intermediate sensitivity. Interestingly, there was a leveling off of viability decline in Normal and $XPB^{+/-}$ cells but not in $XPB^{-/-}$ cells. The differences in the viability trends prompted our investigation of cell cycle changes in the cells following exposure to H_2O_2.

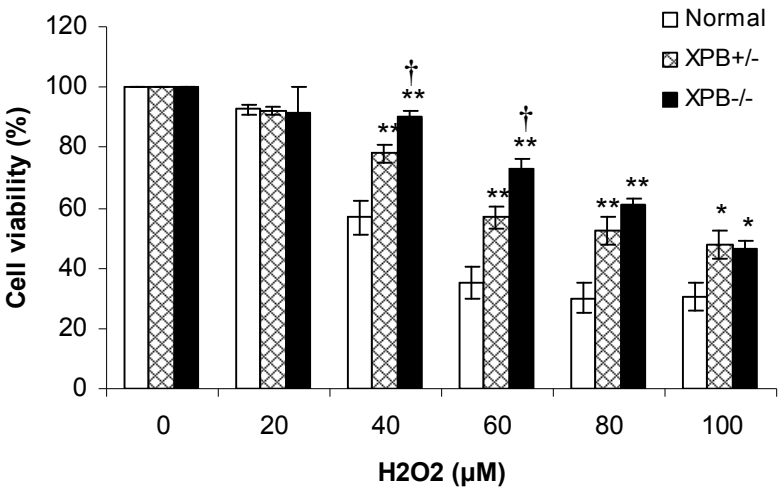

Figure 1: Dose-dependent cell death in H_2O_2 treated cells. $XPB^{-/-}$ and $XPB^{+/-}$ cells are significantly less sensitive to cell death compared to Normal cells at concentrations above 20 µM. *P<0.05; **P<0.01. Two-way ANOVA. Data are represented as mean ± SE. XPB-/- cells are also significantly less sensitive to cell death compared to XPB+/- cells at 40 µM and 60 µM (†P<0.05).

4.2 Dysfunctional XPB causes deficiency in cell cycle checkpoint function

Figure 2A illustrates the cell cycle histograms of Normal, $XPB^{+/-}$ and $XPB^{-/-}$ cells 24 hours after exposure to H_2O_2. Normal cells displayed a dose dependent shift in cell cycle profiles (Fig. 2B). An increase in G2/M phase of cells was accompanied by a decrease in G1 and S phases in the 20 μM and 40 μM H_2O_2. Above 40 μM, the G1 and Sub-G1 populations were greatly increased. $XPB^{+/-}$ cells displayed a similar shift in cell cycle profiles, however there was little increase in the Sub-G1 population (Fig. 2C). $XPB^{-/-}$ cells presented non-significant changes in profiles up to 40 μM. Above this concentration, there was a slight decrease in the G2/M population with concomitant increases in the G1 and Sub-G1 populations (Fig. 2D). To determine if cell cycle profile changes in the cells or lack thereof were associated with DNA damage, we employed the Alkaline Single Cell Electrophoresis or Comet Assay.

A.

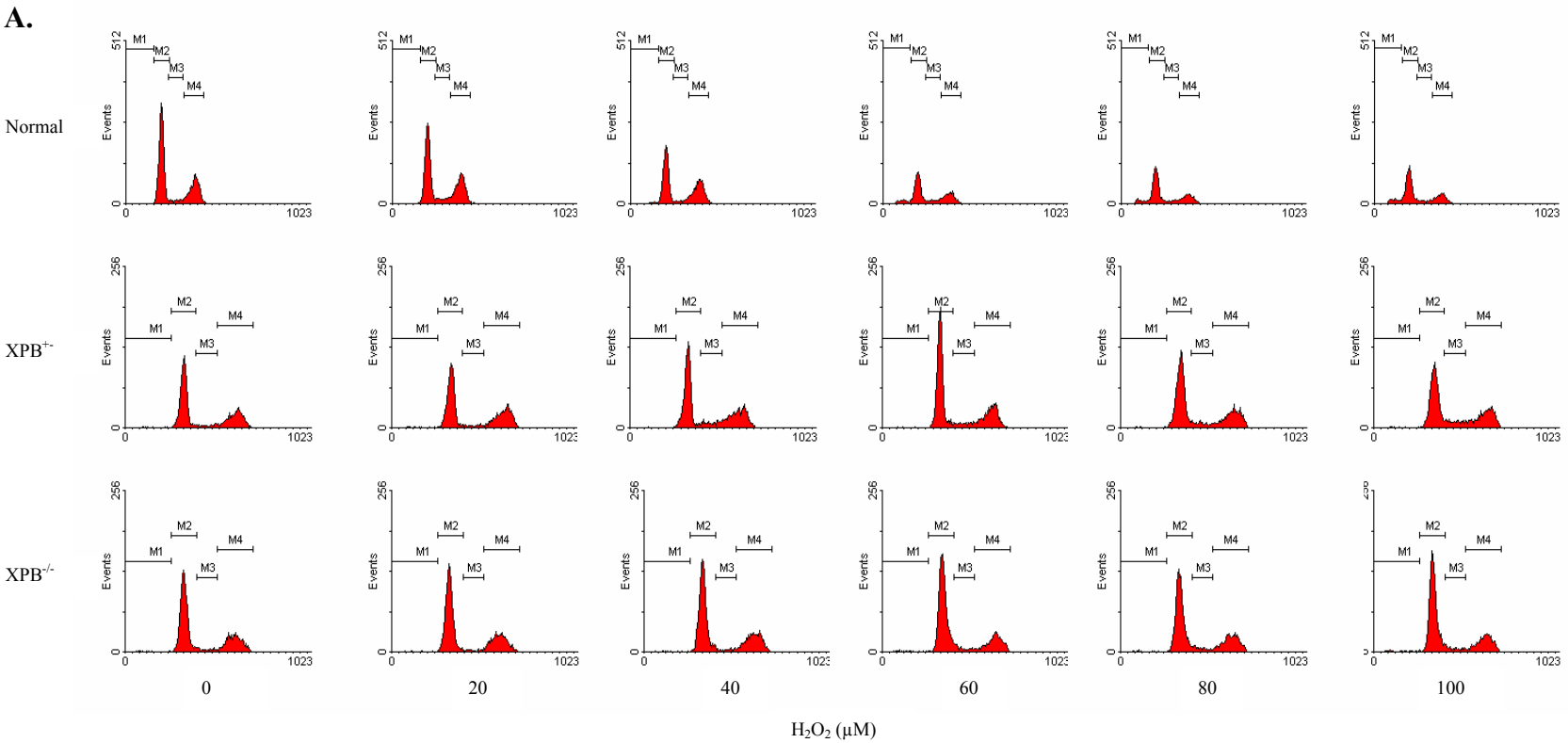

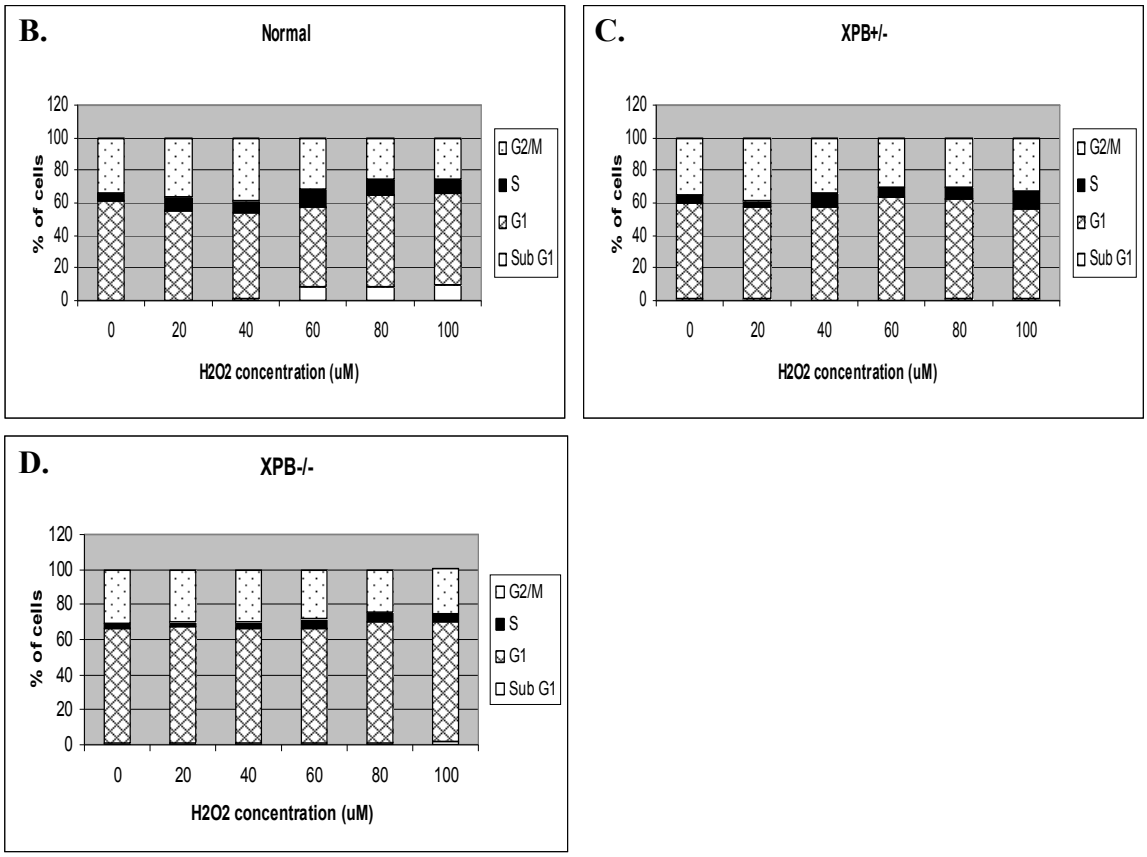

Figure 2: Cell Cycle Analysis by FACS. A. Cell cycle histograms 24 hours after exposure to H_2O_2. Clear profile changes and phase shifts observed in Normal and $XPB^{+/-}$ cells. Changes in $XPB^{-/-}$ cells not easily discriminated. B-C. Percentages of cells in each phase of the cell cycle. B. H_2O_2 effects a G2/M increase at 20 to 40 μM with increases in G1 and sub-G1 populations at subsequent concentrations. C. Similar increase in G2/M followed by G1 populations in $XPB^{+/-}$ cells at the same doses as in Normal cells. Minimal sub-G1 population observed. D. $XPB^{-/-}$ cells do not display the G2/M increase observed for the latter two cells at 20 to 40 μM. G1 and sub-G1 populations increase slightly at subsequent concentrations.

4.3 Dysfunctional XPB compromises repair capacity for oxidative DNA lesions

A pair of single cell gel electrophoresis (Comet) assays was done to determine initial DNA damage 2 hours following H_2O_2 exposure and persisting DNA damage after a 22 hour recovery period. Nuclei with undamaged DNA appear round (Fig. 3A); nuclei with damaged DNA in the form of strand breaks result in DNA fragments which migrate faster during gel electrophoresis and give rise to a "tail" (Fig. 3B). Comet tail moment, a function of tail length and fluorescence intensity, was used as a measure of DNA damage.

At the 2 hour time point, Normal cells displayed significant dose dependent increases ($p<0.05$) in tail moments at concentrations above 60 μM. $XPB^{-/-}$ and $XPB^{+/-}$ cells displayed a similar trend starting with 40 μM. Also, it is noted that Normal cells displayed significantly lower ($p<0.001$) tail moments compared to the other two cell types from 40 μM to 100 μM H_2O_2 (Fig. 3C).

Following the recovery period, there were significant reductions ($p<0.01$) in tail moments in all cells at all concentrations where there were previously significant increases (Fig. 3C). This decrease in tail moment back toward the baseline is indicative of damage repair. Normal and $XPB^{+/-}$ cells displayed no significant difference ($p>0.05$) in post-recovery tail moments between treated and untreated cells, apart from high doses (100 μM for Normal and 80 μM and 100 μM for $XPB^{+/-}$). $XPB^{-/-}$ cells exposed to H_2O_2 retained significantly higher ($p<0.001$) tail moments than untreated cells at all doses apart from 20 μM. Recovered $XPB^{-/-}$ cells also displayed significantly higher tail moments than recovered Normal and $XPB^{+/-}$ cells at 60 to 100 μM. There was no such significant difference ($p>0.05$) between recovered Normal and $XPB^{+/-}$ cells.

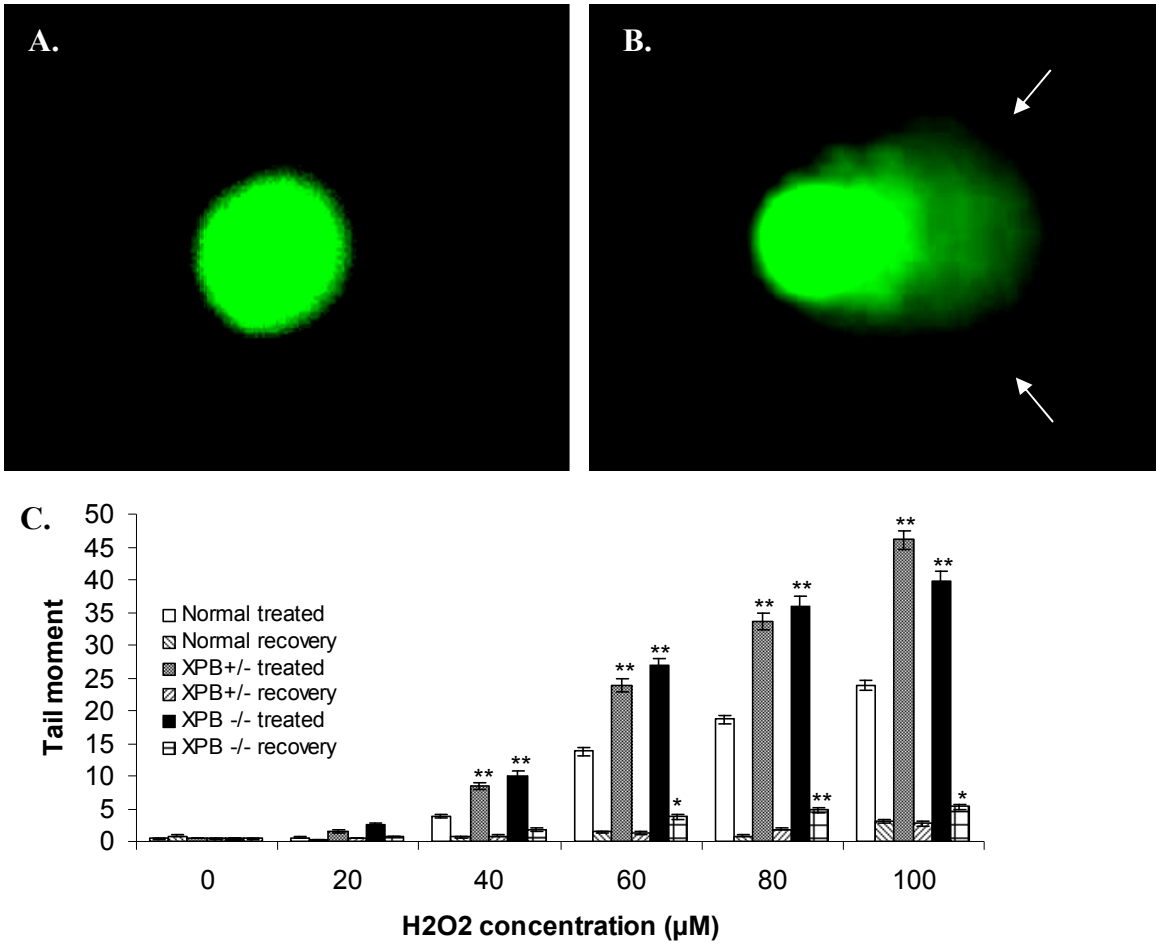

Figure 3: Alkaline Single Cell Gel Electrophoresis. A-B. Nucleic material of cells stained with SYBR green following SCGL. A. Nucleus with no apparent DNA damage. B. Nucleus with DNA damage shown by the presence of a tail (arrows), resulting in the image of a comet. C. Tail moments immediately following 2 hour H2O2 treatment and 22 hour recovery in fresh medium. Treatment of 40 µM H2O2 and above resulted in significantly increased tail moment ($P<0.01$) which decreased significantly following recovery ($P<0.001$) in all cell types. There was no significant difference in moments between all cells for after treatment at 20 µM H_2O_2 ($P>0.05$), however $XPB^{-/-}$ and $XPB^{-/-}$ cells exhibited higher moments compared to the Normal cells at the subsequent concentrations. Following recovery, there was no significant difference between Normal and $XPB^{+/-}$ cells at all concentrations ($P>0.05$) while $XPB^{-/-}$ cells showed significantly higher moments than Normal cells at 60 - 100 µM. *$P<0.05$ and **$P<0.001$ indicate significantly greater tail moment when comparing $XPB^{-/-}$ and XPB^{+-} cells to their Normal counterparts. Two way ANOVA. Data are represented as mean ± SE.

4.4 Dysfunctional XPB increases incidence of oxidative stress induced genomic instability

Micronuclei which are the result of lagging chromosomes and acentric chromosomes being excluded from daughter nuclei following cytokinesis are a marker of genome instability. Utilizing cytochalasin B, an actin polymerization inhibitor, we arrested cells that completed a single nuclear division at cytokinesis. The numbers and distribution of micronuclei in the resulting binucleates were scored to determine genome stability following exposure to H_2O_2 (Fig. 4). Figure 4A and B show differentially stained binucleates without and with the presence of micronuclei. We reduced the H_2O_2 dose range to a maximum of 40 μM as higher concentrations yielded very few mitotic cells and binucleated cells. In congruence to the ability of H_2O_2 to induce DNA strand breaks, all three cell types displayed significant increases in micronuclei frequency following exposure. $XPB^{-/-}$ cells showed significantly higher micronuclei frequency than Normal cells when exposed to H_2O_2 ($p<0.05$). There was no significant difference between $XPB^{+/-}$ and Normal cells or between $XPB^{+/-}$ and $XPB^{-/-}$ cells ($p>0.05$).

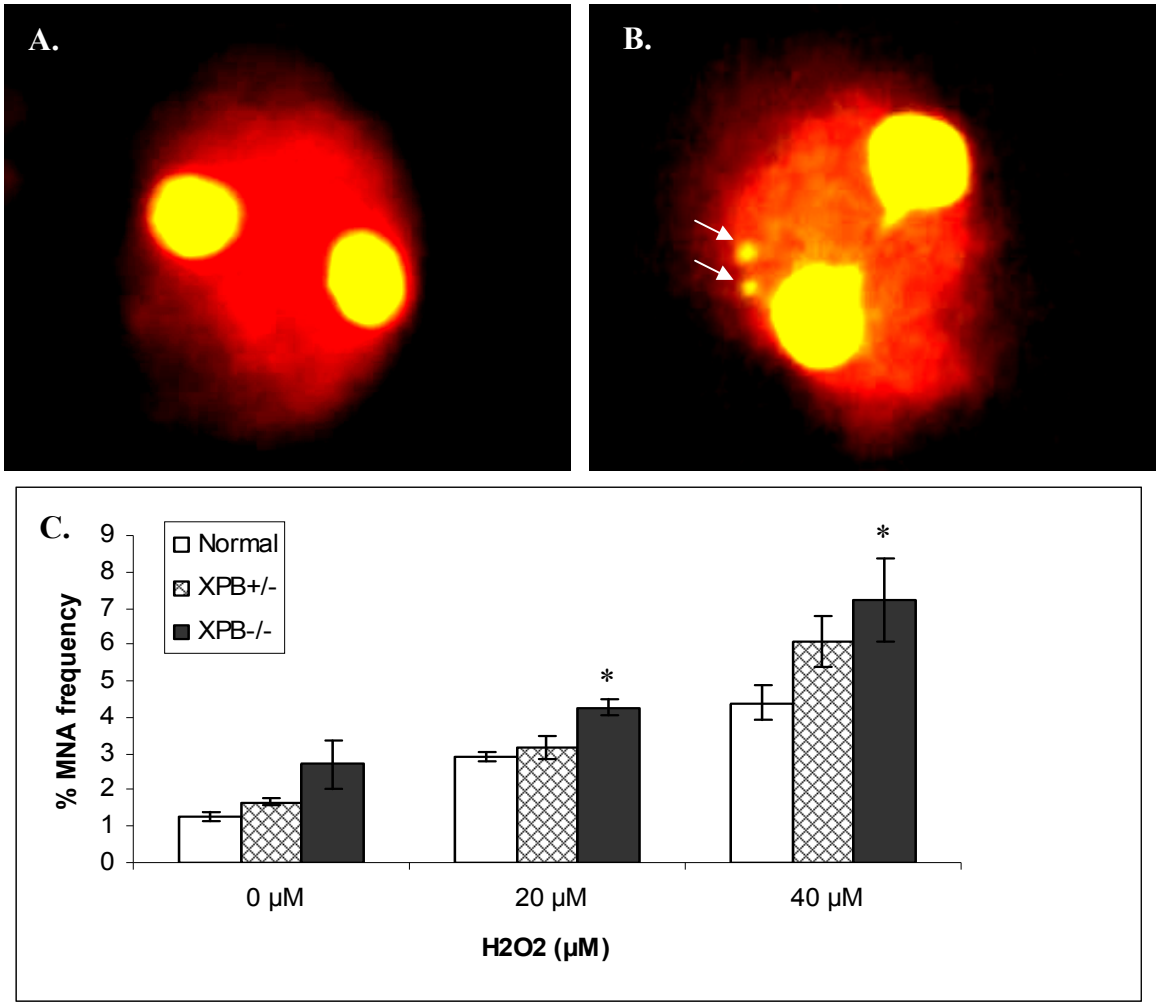

Figure 4: Cytokinesis Blocked Micronucleus Assay. (A-B) Acridine orange-stained cytokinesis blocked binucleated cells (BN). Note the differential staining of cytoplasm (red/orange), and nuclei and micronuclei (grean/yellow) A**.** BN with no micronuclei. B**.** BN with two micronuclei (MN), indicating higher genome instability from loss of DNA fragments (arrows). C. Percent MN per 1000 BN scored following H_2O_2 treatment. There was no significant difference between XPB^{+-} and Normal cells ($P>0.05$). $XPB^{-/-}$ cells exhibit significantly more MN presence in BN cells compared to control cells. *$P<0.05$. Two-way ANOVA. Data are represented as mean ± S.E.

4.5 Dysfunctional XPB results in early appearance of senescent characteristics

Based on the results of the crystal violet assays and cell cycle profiles, we selected a dose of 20 μM to utilize for low dose chronic oxidative stress exposure. This dose caused only slight non-significant decreases in cell viability in all three cell types and did not greatly perturb cell cycle profiles. We also included a set of cells cultured under hyperoxia (40% O_2) for a broader perspective of chronic oxidative stress.

Senescent characteristics included enlarged and flattened cell morphologies, increased cell volume, expression of senescence-associated β-galactosidase (SA-β-gal) and reduced population doubling rate. In the absence of oxidative stress, the enlarged morphologies in $XPB^{-/-}$ cells appeared at day 23 of the study compared to Normal fibroblast morphologies throughout the entire period in Normal cells (Fig. 5A, 5C). SA-β-gal expression in $XPB^{-/-}$ was detected at day 24 compared to nil expression in Normal cells (Fig. 5D, 5F). $XPB^{+/-}$ cells also displayed typical fibroblastic morphologies and nil SA-β-gal expression when not exposed to H_2O_2 or 40% O_2 (Fig. 5B, 5E).

Exposure to oxidative stress conditions resulted in the appearance of senescent characteristics in Normal and $XPB^{+/-}$ cells and hastened their appearance in $XPB^{-/-}$ cells. The latter displayed cell body enlargement as early as day 6 for H_2O_2 and day 11 for 40% oxygen compared to days 9 (H_2O_2) and 17 (40% O_2) for Normal cells and days 11 (H_2O_2) and 21 (40% O_2) for $XPB^{+/-}$ cells (Fig. 5A-5C). SA-β-gal expression in stressed $XPB^{-/-}$ cells was observed by day 12 (Fig. 5D-F). Minimal staining was only observed in H_2O_2 treated Normal and $XPB^{+/-}$ cells by day 18 and absence of staining with 40 O_2. Interestingly, treatment with H_2O_2 results in earlier appearance of senescent morphologies and positive SA-β-gal staining than 40% O_2. With the latter treatment

regime, minimal staining was observed even by the end of the 30 day period. We also observed that $XPB^{+/-}$ cells first manifested senescent morphological changes later than both the other two cell types.

Population doubling rates in treated $XPB^{-/-}$ cells were also slower than those in treated Normal cells. While the Normal cells were able to continue division, albeit with the rate approaching 0 at the end of the 30 day period, $XPB^{-/-}$ cells had a rate close to 0 throughout the treatment period. $XPB^{+/-}$ cells were intermediate in the appearance of these features (Fig. 5G).

A1. Normal

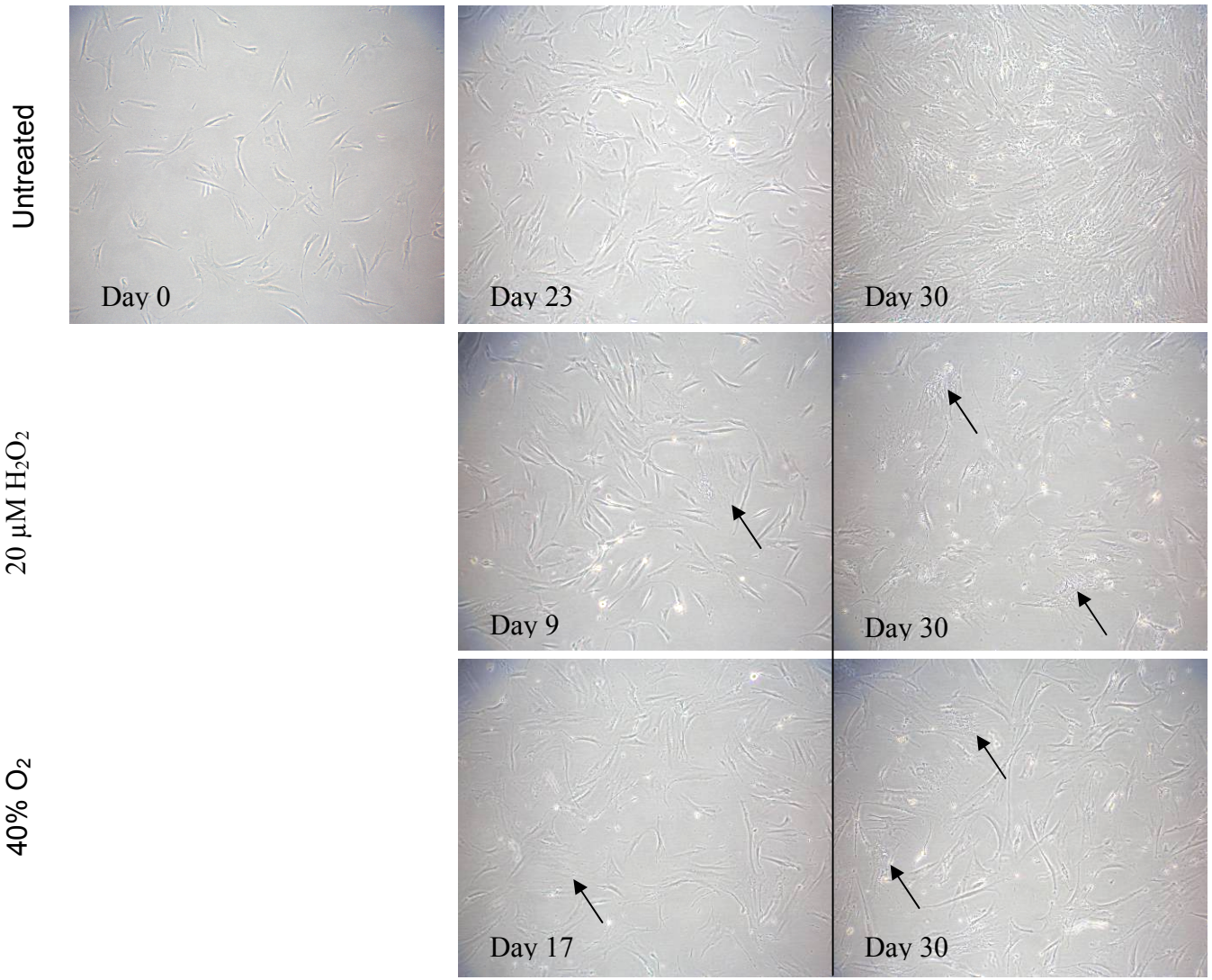
Untreated
20 μM H_2O_2
40% O_2
Day 0
Day 23
Day 30
Day 9
Day 30
Day 17
Day 30

A2. XPB$^{+/-}$

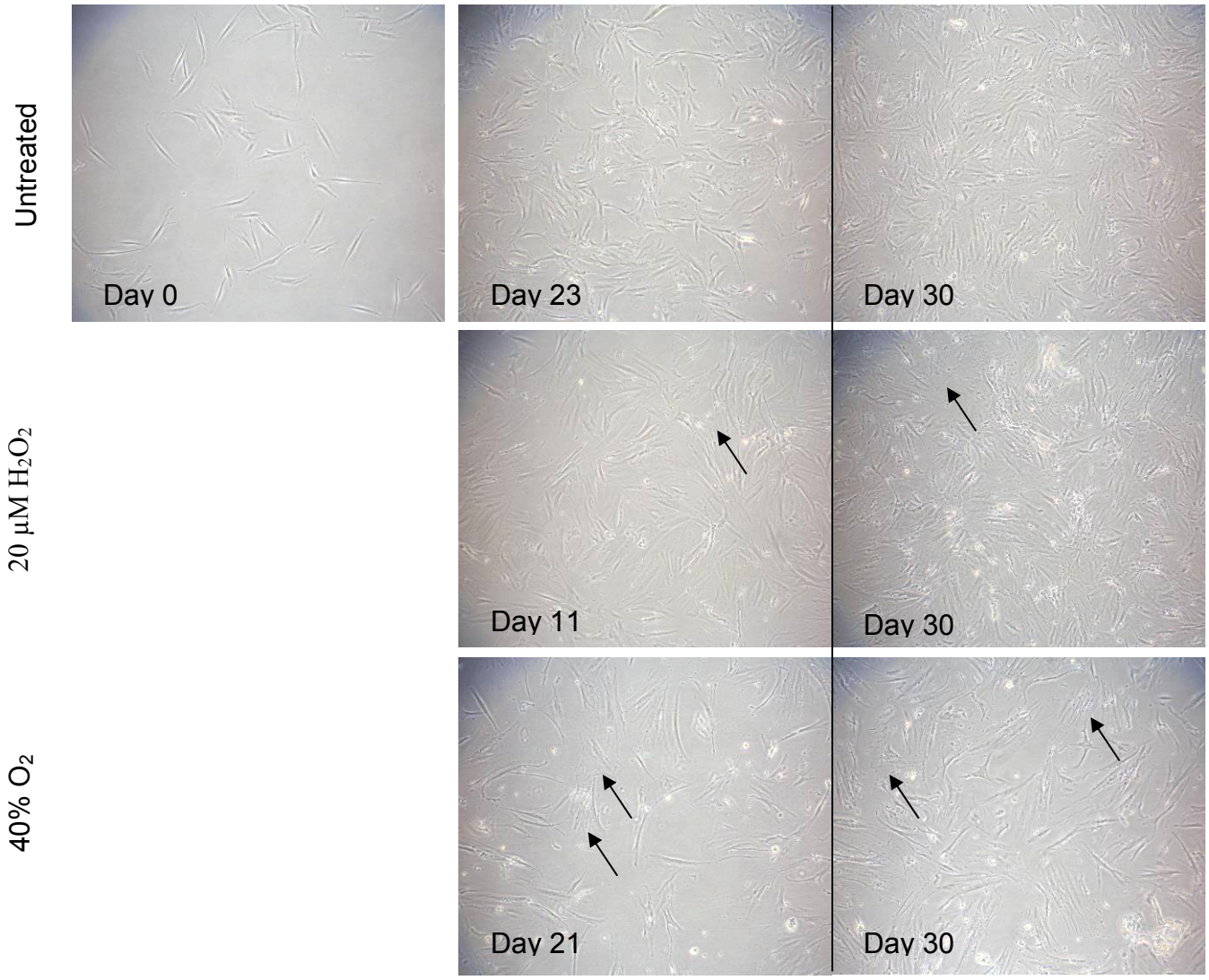
Untreated
20 μM H_2O_2
40% O_2
Day 0
Day 23
Day 30
Day 11
Day 30
Day 21
Day 30

A3. XPB$^{-/-}$

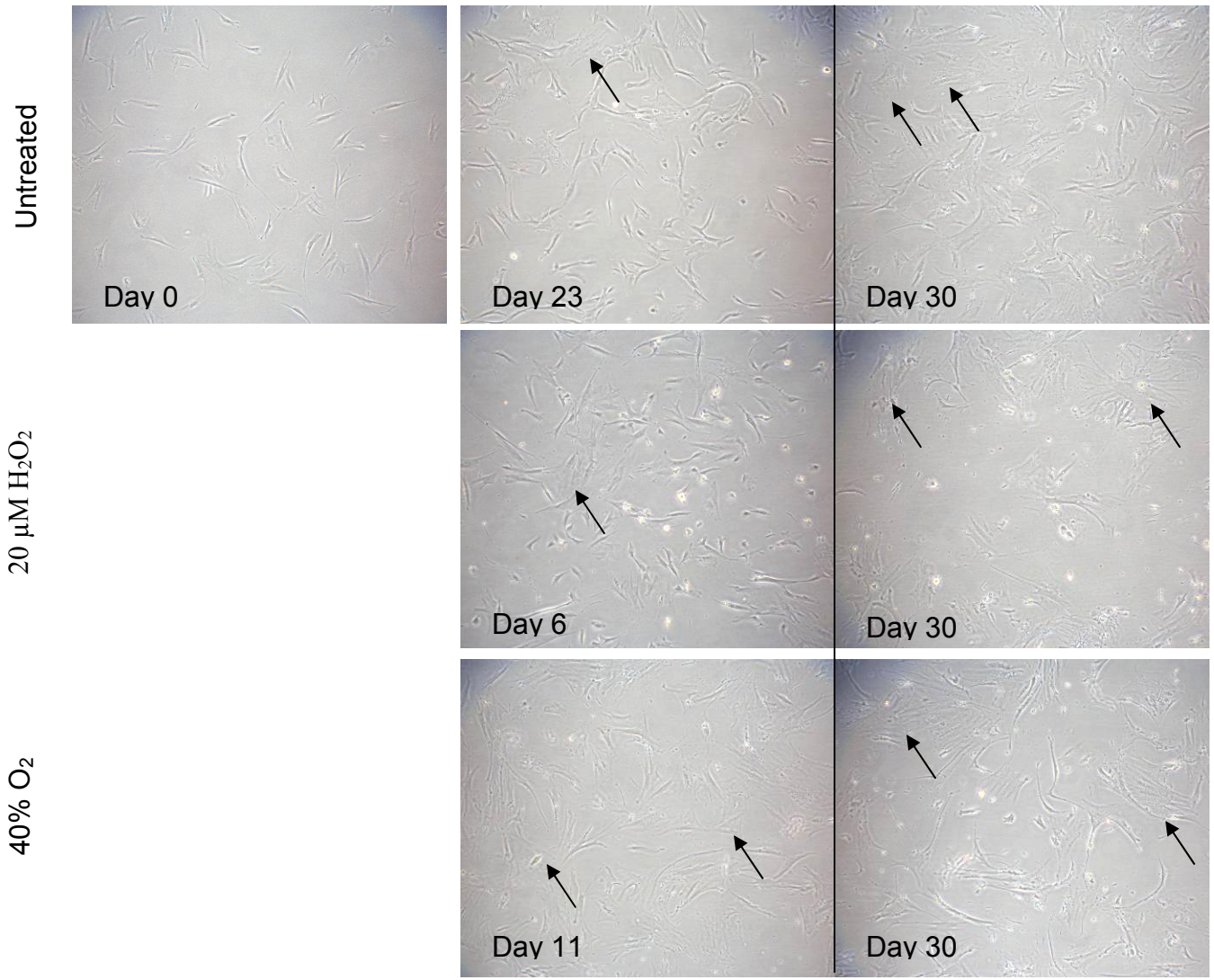
Untreated
20 μM H_2O_2
40% O_2
Day 0
Day 23
Day 30
Day 6
Day 30
Day 11
Day 30

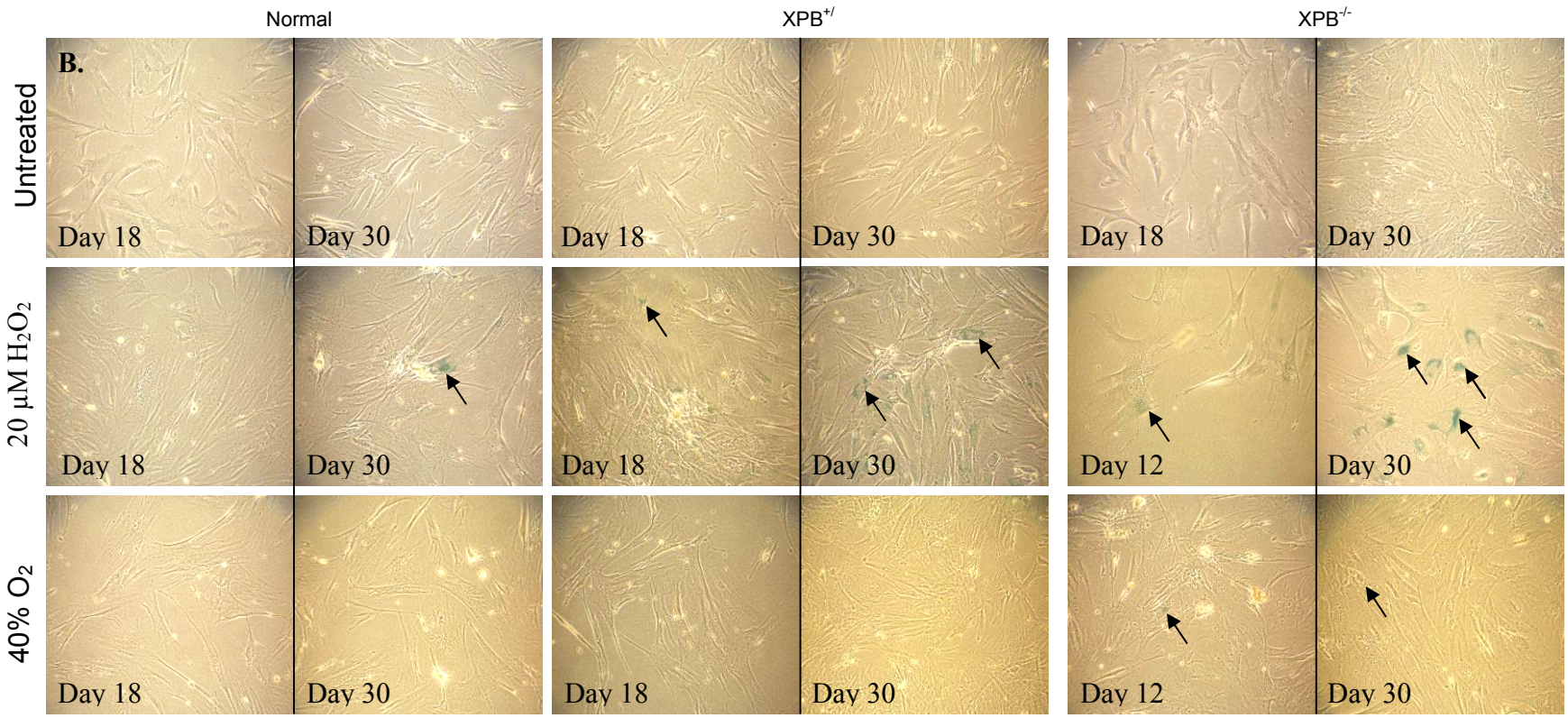
Normal
XPB+/
XPB-/-
B.
Untreated
20 μM H2O2
40% O2
Day 18
Day 30
Day 18
Day 30
Day 18
Day 30
Day 18
Day 30
Day 18
Day 30
Day 12
Day 30
Day 18
Day 30
Day 18
Day 30
Day 12
Day 30

C.

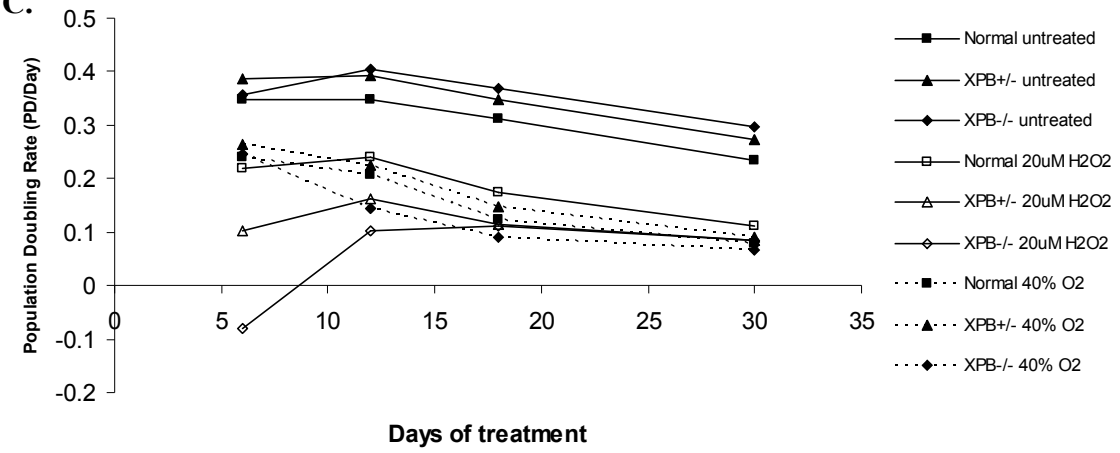

Figure 5: Cellular Kinetics Study. A. Morphologies of fibroblasts under chronic oxidative stress at 40X magnification. Typical elongated fibroblast morphology is replaced with enlarged and flattened senescent morphology (arrows) over time and with oxidative stress. Pictures show cells at the start of treatment, on the first day of morphology change and at the end of treatment. Where no change occurs before the final day, pictures from day 23 are shown. Morphology change takes place earlier in $XPB^{-/-}$ than in the other two cell types in all conditions and hastened by oxidative stress. B. Senescence Associated β-galactosidase Staining. 100X magnification. Pictures show cells on day of first detectable stain and at the end of treatment. Where stain is undetectable before the final day, pictures from day 18 are shown. Positive staining (bluish; arrows) is present earlier for $XPB^{-/-}$ cells than for the other two cell types in all conditions and hastened with oxidative stress. C. Population Doubling Rate. Rate derived by dividing the total number of population doublings on the sampling days by the number of days that have passed. Though, untreated cells also displayed a decline; these were still higher than the rates of treated cells. Treated $XPB^{-/-}$ cells possessed the lowest rates out of all three cell types and displayed rates below 0.1 earlier in the treatment period than Normal and $XPB^{+/-}$ cells.

4.6 Dysfunctional XPB sensitizes telomeres to attrition

All cells under untreated conditions and exposure to H_2O_2 and 40% O_2 displayed telomere shortening as revealed by terminal restriction fragment (TRF) length analysis. Under all conditions, raw decreases in TRF length were greater in $XPB^{+/-}$ and $XPB^{-/-}$ cells than in Normal cells (Fig. 6B). With oxidative stress, there was a decrease in raw TRF length in Normal cells while $XPB^{+/-}$ and $XPB^{-/-}$ cells showed no apparent changes (Fig. 6B).

As telomere loss is a factor of cell division, population doubling was considered. After taking into account population doubling numbers for all samples, $XPB^{-/-}$ and $XPB^{+/-}$ cells exhibited substantially greater telomere attrition rates (TRF length decreases divided by population doubling numbers) than Normal cells under all conditions. In both untreated cells and cell treated with 20 μM H_2O_2, $XPB^{+/-}$ and $XPB^{-/-}$ cells displayed an approximately three-fold increase in telomere attrition rates compared to Normal cells. At 40% O_2, the telomere attrition rate of $XPB^{+/-}$ cells was slightly elevated compared to Normal cells but 1.8-fold greater in $XPB^{-/-}$ cells relative to Normal cells (Fig. 6C).

A.

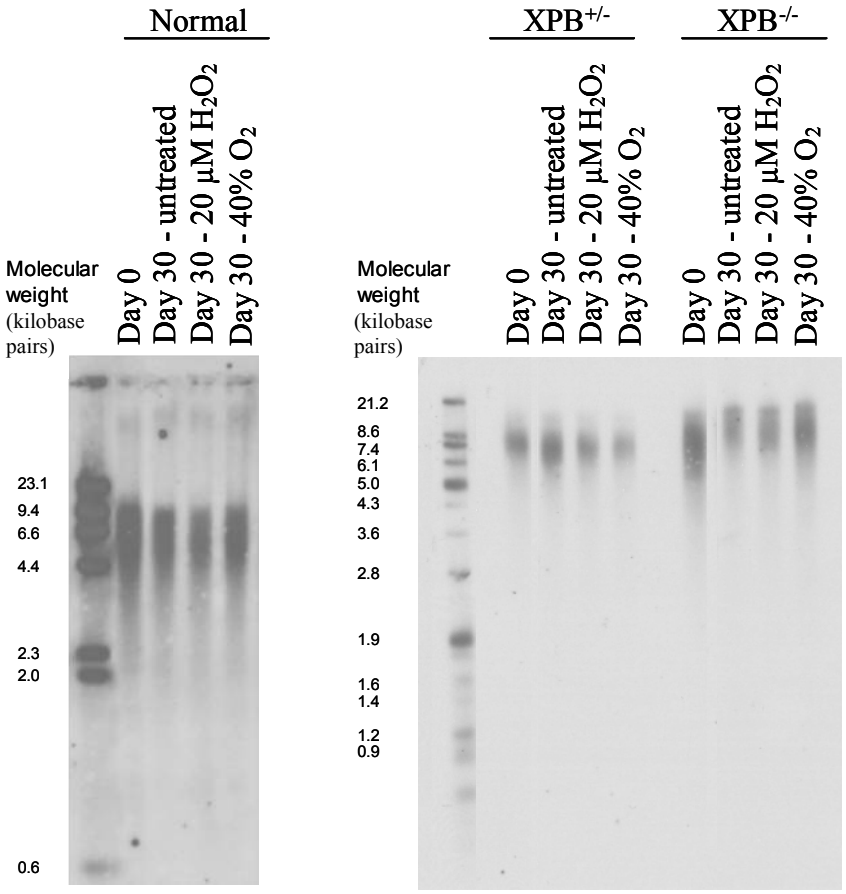
Normal
XPB+/-
XPB-/-
Day 0
Day 30 - untreated
Day 30 - 20 µM H2O2
Day 30 - 40% O2
Molecular weight (kilobase pairs)
23.1
9.4
6.6
4.4
2.3
2.0
0.6
21.2
8.6
7.4
6.1
5.0
4.3
3.6
2.8
1.9
1.6
1.4
1.2
0.9

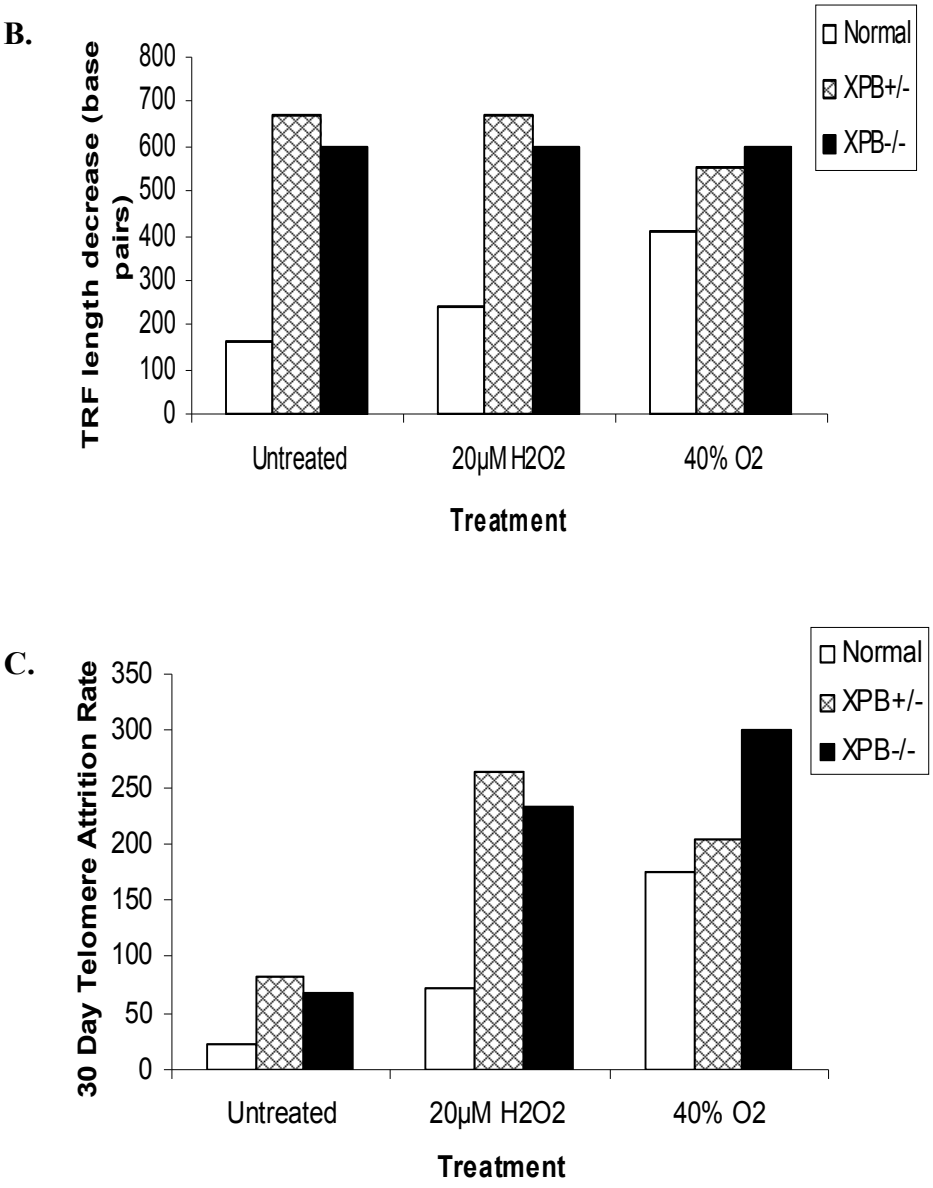

Figure 6: Telomere Restriction Fragment Analysis A. Southern blot of telomere restriction fragments obtained by digest of genomic DNA with Hinf1 and RsaI. B. Total TRF length decreases after completion of 30 day period. Both XPB deficient cell types displayed greater decreases of TRF length than Normal cells under all conditions. C. Telomere attrition rate derived by dividing the TRF length decrease by the number of population doublings. Attrition rate increases in all cell types under conditions of oxidative stress. Similar trend to raw TRF length decrease was seen. XPB deficient cell types exhibited a greater attrition rate than Normal cells. Attrition rate for $XPB^{=/-}$ was also markedly greater than that for $XPB^{+/-}$ cells at 40% O_2.

4.7 XPB upregulation occurs as part of normal cellular response to oxidative stress

In Normal cells, upregulation of XPB is evident at 24 hours after treatment and levels subsequently returned to control levels. p53 phosphorylation increased within 2 hours and p53 upregulation was observed at 24 hours; both levels returned to control levels at 48 hours. p21 upregulation was noted at 24 hours and persisted at 48 hours (Fig. 7A). Similarly, upregulation of XPB occurred in $XPB^{+/-}$ cells at 2 hours with return to control levels at 24 and 48 hours. Phosphorylation and upregulation of p53 was observed at 2 hours and persisted till 48 hours. p21 upregulation was detected till 48 hours (Fig. 7B). XPB expression patterns were difficult to ascertain accurately in $XPB^{-/-}$ cells. p53 upregulation was seen at 2 hours while increased phosphorylation levels were observed at 24 hours; both persisted till 48 hours. p21 upregulation persisted till 48 hours (Fig. 7C).

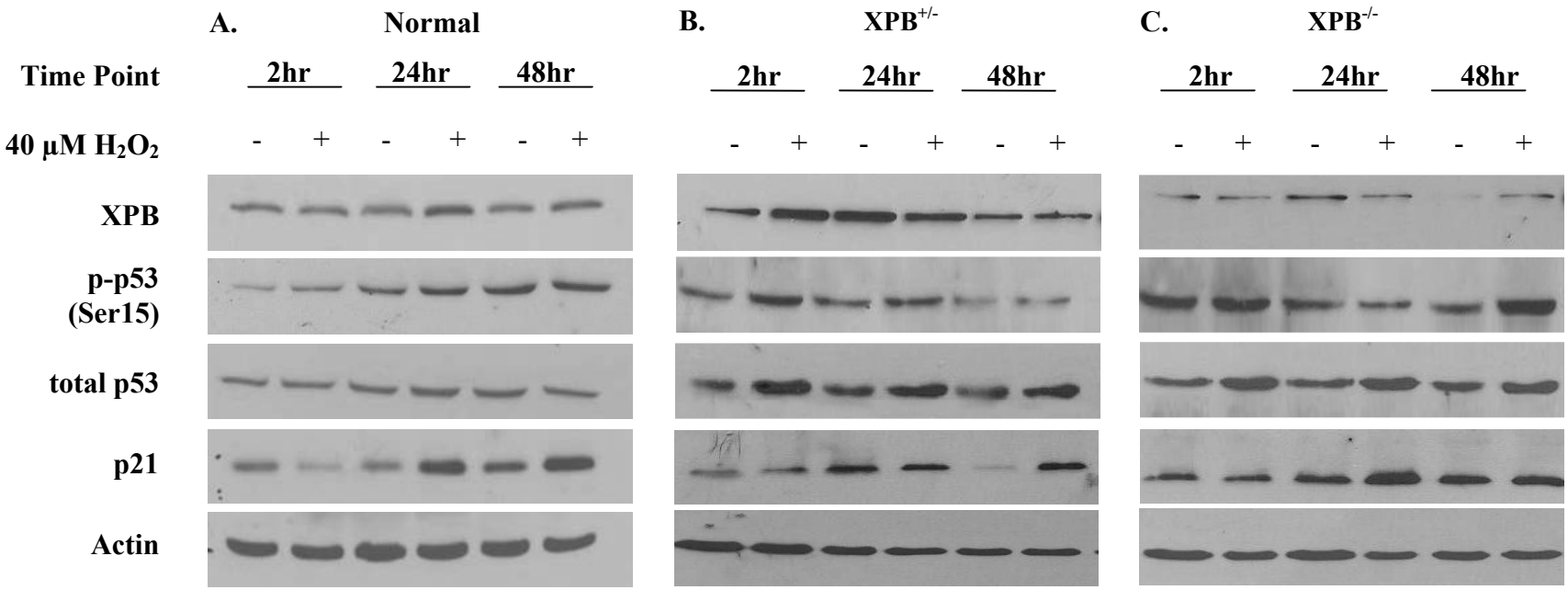

Figure 7: Western Blot. A. Normal cells. Treatment with H_2O_2 results in upregulation of XPB and phosphorylation followed by upregulation of p53. B. $XPB^{+/-}$ cells. XPB upregulation occurs as was observed in Normal cells. p53 upregulation takes place at an earlier time point (2 hours) and persists till 48 hours. C. $XPB^{-/-}$ cells. p53 phosphorylation is delayed till 48 hours; upregulation persists till 48 hours.

4.8 XPB forms foci in HeLa cells which reduce in number following oxidative stress

Foci which were positive for XPB were observed in HeLa cells both in untreated cells and cells exposed to H_2O_2 for 30 minutes (Fig. 8A and 8B). The numbers of large and distinct XPB foci per cell was reduced upon H_2O_2 treatment by 0.6 fold (Fig. 8C) ($P<0.05$). The percentage of cells bearing these foci was also decreased in treated cells by 0.5 fold (Fig. 8D) ($P<0.05$).

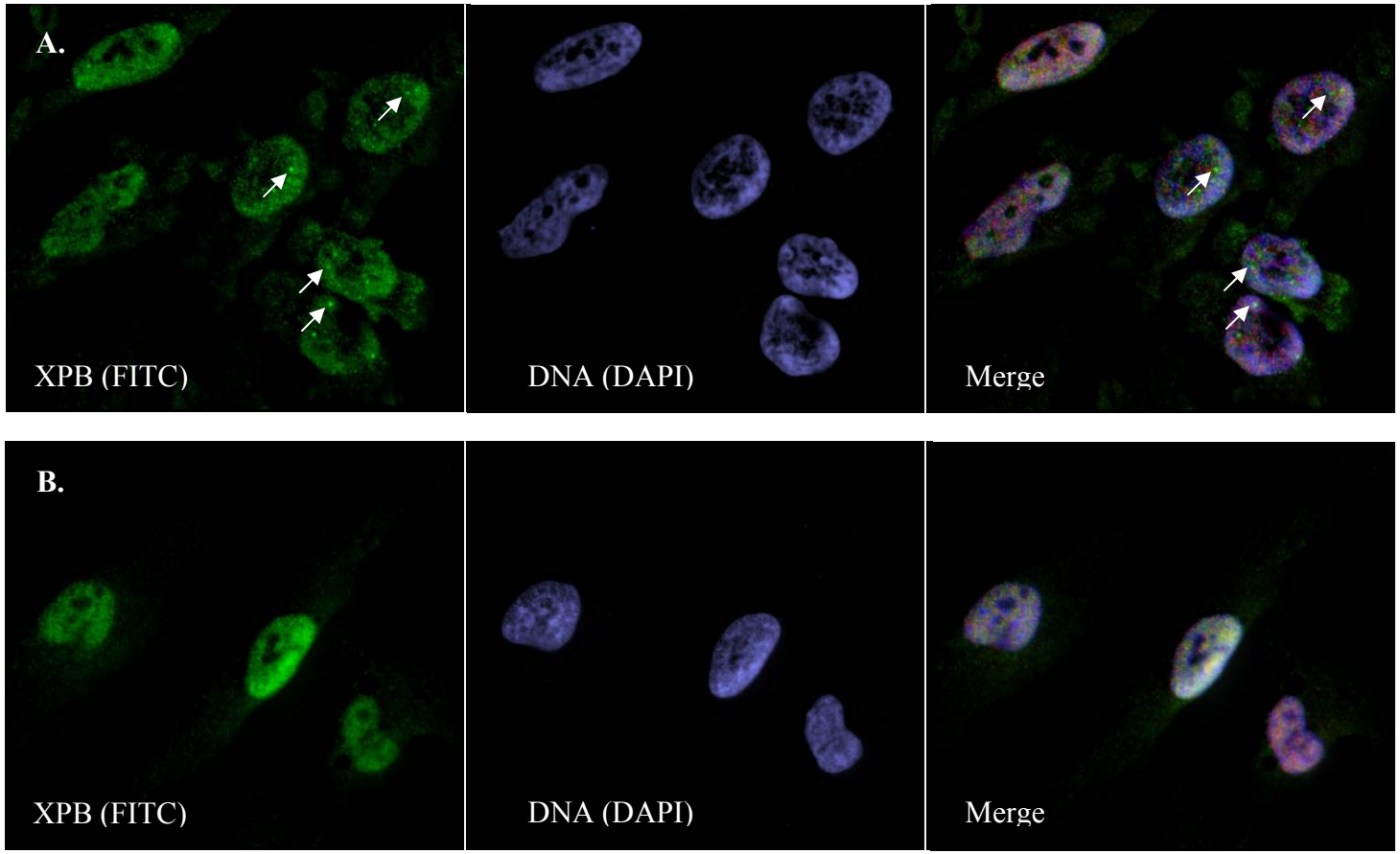
A.
XPB (FITC)
DNA (DAPI)
Merge
B.
XPB (FITC)
DNA (DAPI)
Merge

C.

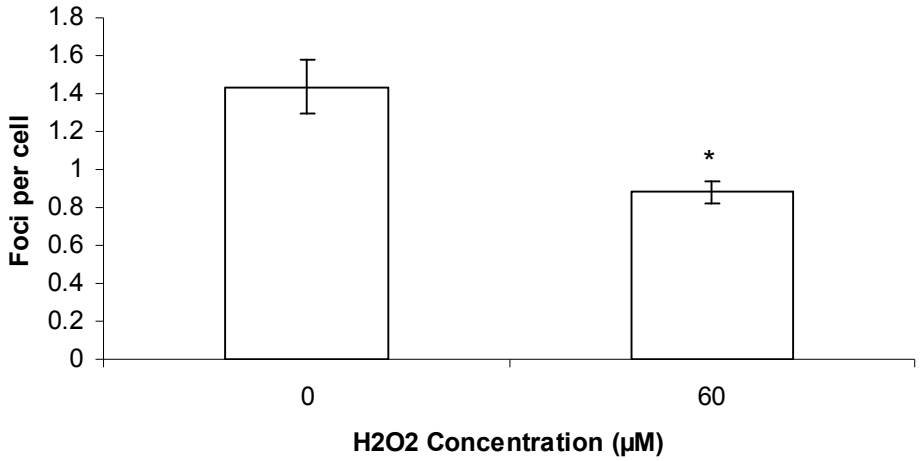

D.

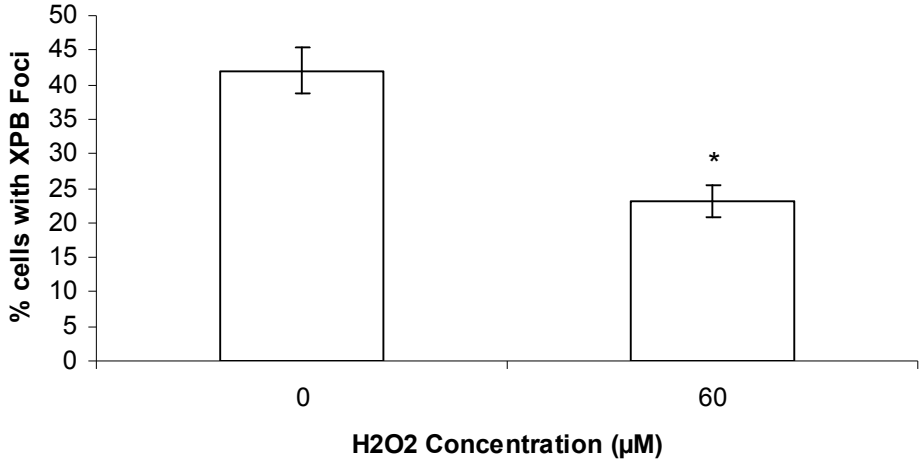

Figure 8: Immunofluorescence on HeLa cells exposed to 60 µM H_2O_2 for 30 minutes. A. Control cells showing XPB foci (white arrows). B. Treated cells showing lack of XPB foci. C. XPB foci distribution in terms of foci per cell. D. Foci distribution in terms of proportion of cells with foci. Less foci were observed in treated cells as compared to controls ($P<0.05$) and more cells with foci were observed in control samples ($P<0.05$). Data are represented as mean ± SE.

4.9 XPB shows no co-localization with either TRF2 or telomeres before or after oxidative stress

Double immunostaining for TRF2 and XPB did not detect co-localization of these two proteins in HeLa cells, independent of H_2O_2 treatment status (Fig. 9A). Likewise, immunostaining for XPB in conjunction with fluorescence *in situ* hybridization with telomere specific probes did not reveal localization of XPB to telomeres in control and H_2O_2 treated HeLa cells (Fig. 9B).

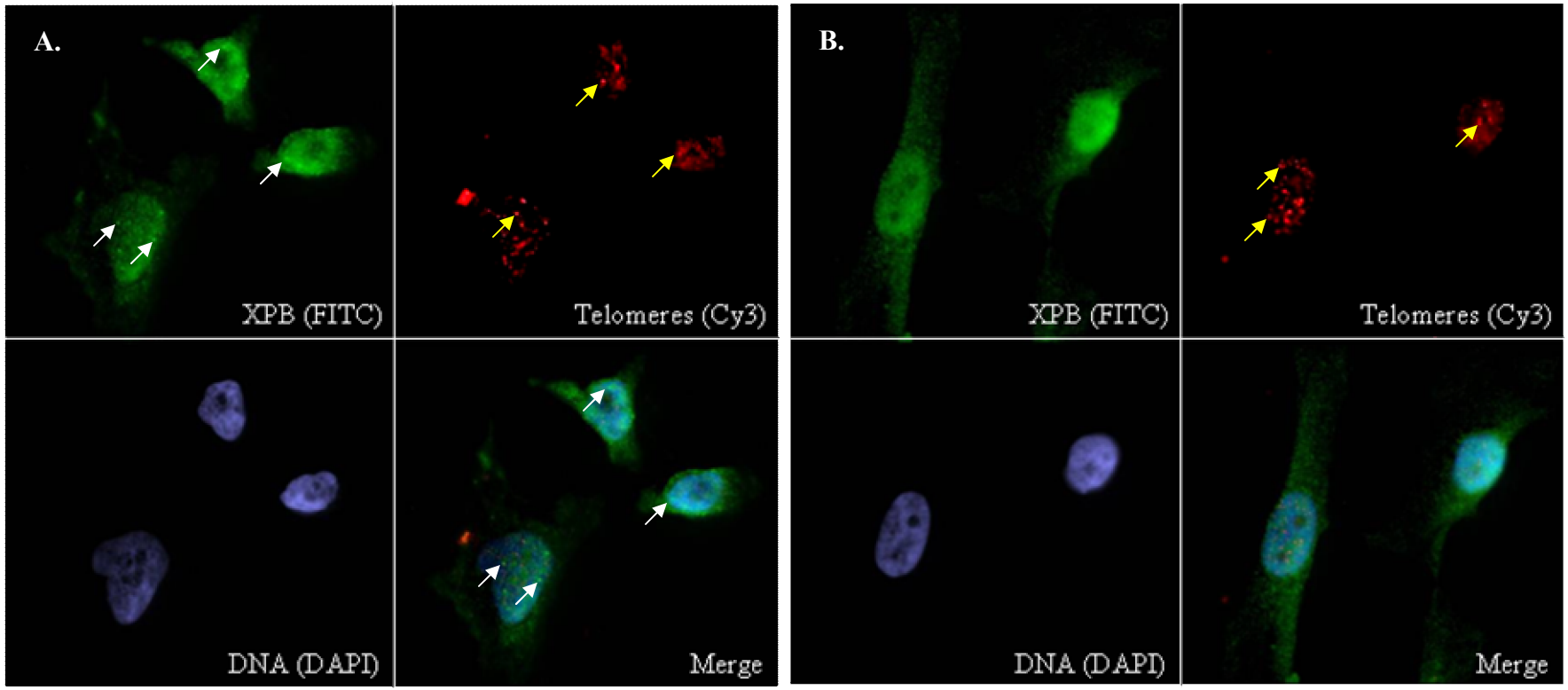

Figure 9A-B: Immunofluorescence-Fluorescence *in situ* hybridization (FISH) on HeLa cells exposed to 60 μM H_2O_2 for 30 minutes. A. Control cells. B. Treated cells. Green XPB foci are indicated by white arrows; red telomere signals are indicated by yellow arrows. No colocalization of XPB and telomeres (yellow foci) observed in cells under both conditions.

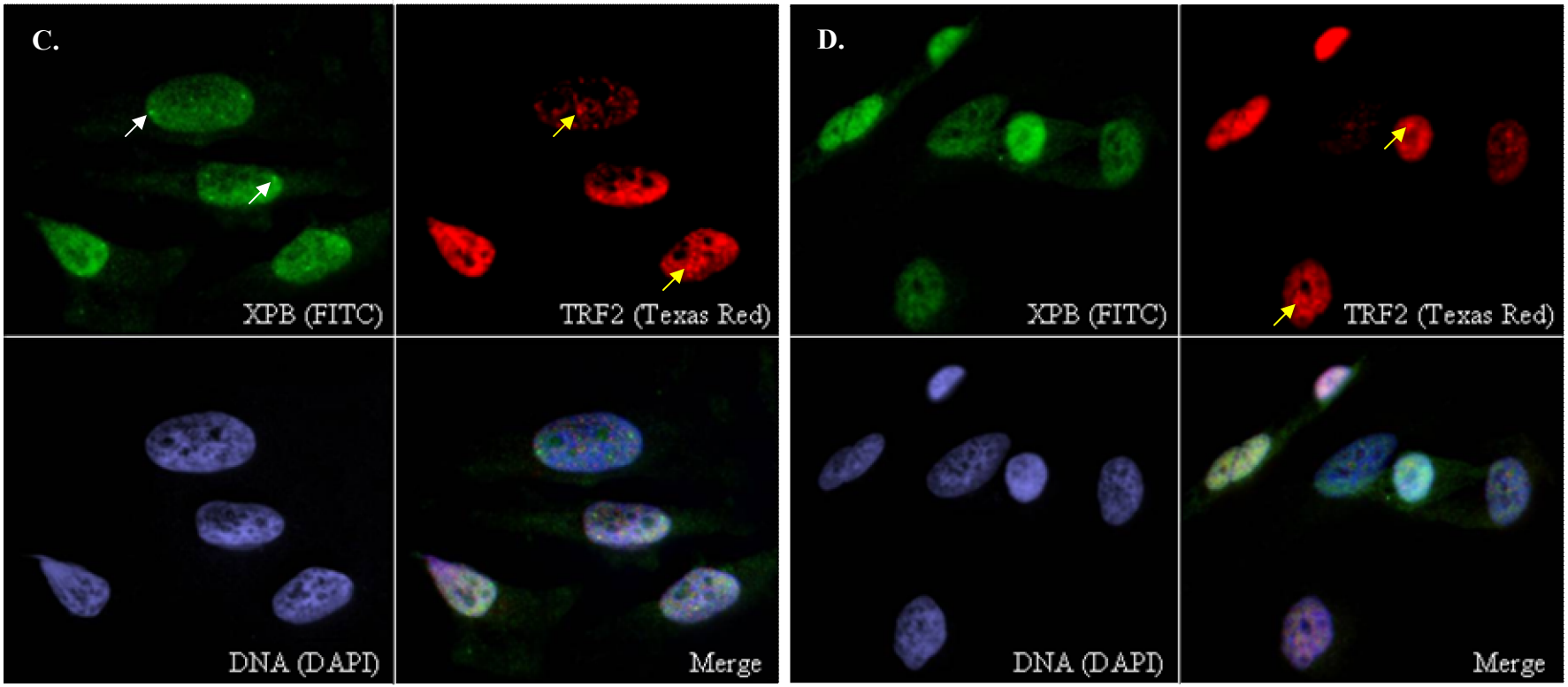

Figure 9C-D: Double Immunofluorescence on HeLa cells exposed to 60 µM H_2O_2 for 30 minutes. A. Control cells. B. Treated cells. Green XPB foci are indicated by white arrows; red TRF2 foci are indicated by yellow arrows.
No colocalization of XPB and telomeres (yellow foci) observed in cells under both conditions.

4.10 XPB does not interact with p53 or phosphorylated p53 *in vivo*

Lymphoblastoid cells derived from a normal individual were treated with 40 μM H_2O_2 for 2 hours. Following this, whole cell lysates were prepared using non denaturing lysis buffer. Western blots carried out on these lysates showed similar patterns of XPB upregulation as well as p53 phosphorylation and upregulation as observed in fibroblasts cells (Fig. 10A). Co-immunoprecipitation with XPB as the bait protein using anti-XPB IgG did not show the presence of p53 or p-p53. It was noted p-p53 probing revealed bands under both IP conditions, including that utilizing control IgG. These bands are likely a result of non-specific activity of the p-p53 antibody as the control IgG displayed no bands for either XPB or more importantly, p53. If p-p53 were indeed present in the IP product, probing with the more specific and sensitive p53 DO-1 antibody would have also detected it as part of total p53. Total p53 was however, undetected. As a control for the protocol, XPD, a known interacting partner of XPB was detected (Fig. 10B). The reciprocal experiment using p53 and p-p53 as bait proteins likewise did not co-immunoprecipitate XPB. The large amounts of p-p53 in the p53 pulldown lanes were due to increased film exposure time as result of the low sensitivity of the p-p53 antibody. The higher sensitivity of the p53 DO-1 antibody in this reciprocal experiment also contributed to the larger amounts of p-p53 being precipitated by it than by the p-p53 antibody (Fig. 10C).

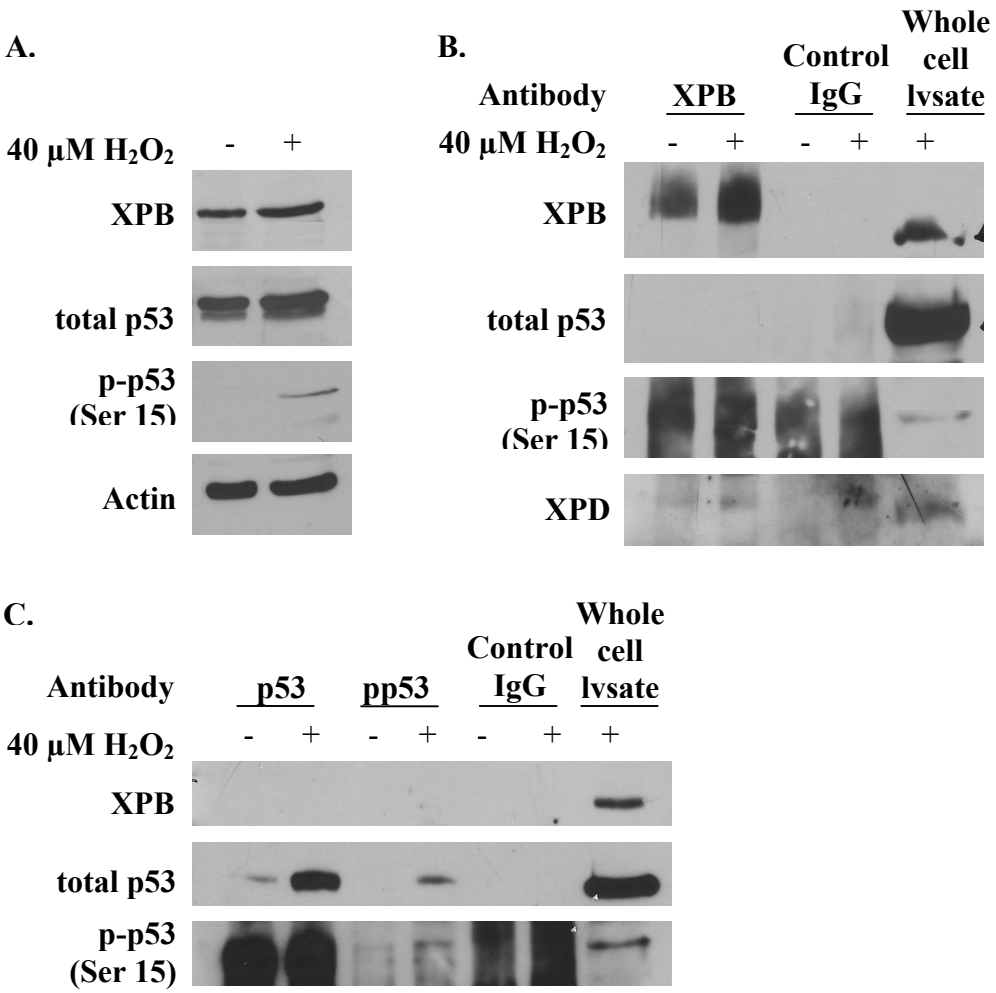

Figure 10: Co-immunoprecipitation on Normal human lymphoblastoid cells exposed to 40 μM H_2O_2 for 2 hours. A. Whole cell lysates. Similar pattern of XPB upregulation and p53 upregulation and phosphorylation upon H_2O_2 treatment as seen in fibroblast cells. B. Co-immunoprecipitation using XPB as bait protein. Pulldown for p53 and phospho-p53 absent. Pulldown for XPD present. C. Reciprocal experiment of B.; co-immunoprecipitation using p53 and phospho-p53 as bait protein. XPB pulldown absent.

CHAPTER 5

DISCUSSION

DISCUSSION

It is known that the nucleotide excision repair pathway has a function in the repair of DNA lesions induced by oxidative stress. The specifics of this mechanism are however still not clearly understood (Hoeijmakers, 2001). This study aimed to investigate the involvement of the NER factor XPB, a helicase domain containing protein, in oxidative DNA lesion repair.

Our investigations into how XPB dysfunction affects cell viability and cell cycle checkpoints yielded interesting results. $XPB^{-/-}$ cells were significantly more resistant to viability decline than Normal cells. The ability of $XPB^{-/-}$ to survive in spite of oxidative damage hinted at possible cell cycle checkpoint dysfunction. Though subtle, the cell cycle profile changes observed in Normal and $XPB^{+/-}$ fibroblasts were not displayed by $XPB^{-/-}$ cells and any form of checkpoint dysfunction is a major risk factor in oncogenic transformation. Obligatory cell cycle arrest takes place when DNA is damaged so as to allow repair or execution of apoptosis if the damage is irreparable. Cell cycle profile shifts upon exposure to genotoxic agents such as H_2O_2 are thus indications of DNA damage checkpoint activation (Barzilai and Yamamoto, 2004; Iliakis et al., 2003; Shackelford et al., 2000). It is possible that the changes might occur only at higher concentrations of H_2O_2 or that they might take longer to occur in $XPB^{-/-}$ cells. In both of these scenarios, the divergence in cell cycle profile changes in $XPB^{-/-}$ fibroblasts points to a cell cycle dysfunction. It was recently reported that XPB has a partially redundant role in p53-mediated apoptosis signalling (Spillare et al., 2006; Bernstein et al., 2002) and has a relationship with p21 (Hu et al., 2006). The partial redundancy is a possible factor for the subtle differences in cell cycle profiles observed. Complete cell cycle dysfunction in

$XPB^{-/-}$ would be circumvented by other intact pathways in these cells. Our results of high cell viability and checkpoint dysfunction in $XPB^{-/-}$ fibroblasts corroborate these finding, as does the observation that $XPB^{+/-}$ cells display intermediate changes in the cell cycle profile following H_2O_2 exposure. This is significant in light of XPB dysfunction already compromising cell cycle checkpoint response to UV induced DNA damage (Marini et al., 2006); there is now also evidence of a checkpoint dysfunction in response to oxidative lesions.

In addition to the above mentioned report of a role in apoptosis signalling, XPB is well established as a DNA repair factor (Hoeijmakers, 2001). There is an implication that in $XPB^{-/-}$ fibroblasts, the large proportions of cells which have sustained genomic assault and survived also fail to properly repair the damage and can pass this onto progeny. To investigate this possibility, we utilized alkaline single cell gel electrophoresis or Comet assay. This assay allows resolution of single strand breaks in DNA which are known to be induced by H_2O_2. The breaks result in fragments that manifest as a tail due to their faster migration under an electric field. One of the parameters for measuring DNA damage in the Comet assay is tail moment which is a function of tail length and fluorescence intensity (Collins, 2004). Aside from measuring DNA damage, the Comet assay allows inference of repair of this damage if comets from different time points are analysed. Decreases in tail moments at the second time point would imply repair (Duan et al., 2005). We measured tail moments at two time points; immediately after the 2 hour exposure period and 22 hours after removal of H_2O_2. All cells displayed increased tail moments at the 2 hour mark which subsequently decreased after the recovery period. Such a reduction is within expectations as all three cell types have a functional base

excision repair pathway, the main pathway for alleviating oxidative DNA lesions. Notably, while Normal and $XPB^{+/-}$ fibroblasts were able to decrease tail moments close to baseline values, $XPB^{-/-}$ cells retained higher damage after recovery. This is in line with our hypothesis that XPB is involved in proper cellular response to and repair of oxidative lesions. The unrepaired damage in $XPB^{-/-}$ cells could constitute two functional scenarios. The first is that this damage arises from a subset of oxidative lesions that are specifically or preferentially repaired by XPB and its partner factors (Satoh et al., 1993). The second is that XPB and its partner proteins act in concert with the BER to expedite repair of oxidative DNA lesions and XPB dysfunction causes a delay in repair. Our results do not allow us to determine which of these the actual scenario is. The exhibition of higher tail moments by $XPB^{+/-}$ and $XPB^{-/-}$ fibroblasts immediately after H_2O_2 exposure is another interesting trend as it might signify a role for XPB in detecting initial oxidative damage, restricting its extent or starting the repair process. The latter role appears to be more feasible as earlier studies demonstrated that XPB is important for proper recruitment of other NER factors to UV lesion sites (Oh et al., 2007) and that the particular mutation (F99S) in our reduces opening of DNA surrounding UV induced lesions (Coin et al., 2007).

Various syndromes including XP, Ataxia Telangiectasia, Werner syndrome and Bloom syndrome are caused by DNA repair deficiencies and result in increased disposition to cancers (Hoeijmakers, 2001; Norgauer et al., 2003; McKinnon, 2004; Orren, 2006; mor-Gueret, 2006). Lack of or compromised repair in such cells may result in inheritance of DNA damage by their progeny. DNA damage such as chromosomal breaks can result in truncated proteins or fusion proteins with possible loss of function or

down-regulation of tumour suppressors and up-regulation of oncogenes (Hande et al., 1999a; Slijepcevic et al., 1997). Such a process is thus potentially oncogenic. By virtue of detecting such a repair dysfunction in our Comet analyses, we proceeded to examine whether this leads to an outcome of genomic instability. The cytokinesis blocked micronucleus assay measures genome instability using micronuclei as a biomarker. Micronuclei are produced in binucleated cells due to whole lagging chromosomes that fail to attach to the mitotic spindle, or from acentric chromosomal fragments resulting from breaks from the parent chromosome. The consequence of these occurrences is loss of genes since at least part of a chromosome fails to incorporate into the daughter nuclei. These chromosomal fragments give rise to micronuclei which are extruded upon cytokinesis (Fenech, 2000; Hande et al., 1996). Exposure to oxidative stress induced by H_2O_2 resulted in increased micronuclei frequency which is an expected result as H_2O_2 induces DNA strand breaks. It is notable that this frequency is greater in $XPB^{-/-}$ cells than the other two cell types, with $XPB^{+/-}$ cells showing intermediate frequencies. The results from this assay indicate that lack of repair combined with cell cycle checkpoint dysfunction contributes to increased numbers of daughter cells with genomic damage. This agrees with XP-B patients having increased predispositions to developing cancers and implicates oxidative stress as a contributing factor in carcinogenesis in these patients.

It has been widely shown that oxidative stress causes outcomes such as decline in cell viability, cell cycle arrest and DNA damage including enhanced telomere attrition (Duan et al., 2005; von Zglinicki, 2002) and our results have corroborated these findings. Induction of oxidative stress affects the proliferative capacity of cells and predisposes premature senescence and aging. However, the type of stresses faced under physiological

conditions is not a short-term phenomena but rather chronic long term exposure. Notably, cells defective in repair mechanisms such as ataxia telangiectasia have been shown to exhibit a faster rate of telomere attrition and senescence earlier in culture than normal cells (Lee et al., 2005; Tchirkov and Lansdorp, 2003). We performed a group of cellular kinetics studies to address the effects of chronic low level exposure to oxidative stress in relation to XPB.

Replicative senescence is an *in vivo* phenomenon in finite cell cultures (Hayflick and Moorhead, 1961). It is characterized by traits such as an enlarged and flattened cell morphology (Kumazaki et al., 1991), senescence-associated beta-galactosidase (SA-β-gal) expression and reduced population doubling rates. Untreated $XPB^{-/-}$ cells displayed these characteristics towards the end of the study period whereas Normal and $XPB^{+/-}$ cells did not. This is significant as it not only agrees with the segmental progeria presented by XP patients, it implicates factors other than UV for this symptom as cell cultures were not exposed to UV sources for substantial time periods. Consistent with known findings that H_2O_2 and hyperoxia induces premature senescence in cells (Chen and Ames, 1994; Duan et al., 2005), we observed senescent characteristics in our stressed cultures. Oxidative stress induced by both H_2O_2 and 40% O_2 resulted in morphological changes and SA-β-gal expression in all three cell types. Similar to untreated cells, these changes appeared in $XPB^{-/-}$ cells before Normal and $XPB^{+/-}$ cells. As such, the results implicate oxidative stress as a contributing factor for the segmental progeria XP patients suffer from and XPB as a factor in preventing this physiological outcome.

We observed that H_2O_2 had a more pronounced effect on all three cell types than 40% O_2. H_2O_2 is only one of a plethora of reactive oxygen species generated under

normal metabolism. Introduction of exogenous H_2O_2 may thus constitute a greater imbalance in cellular redox potential than hyperoxia which may in turn give rise to more pronounced effects. We also found that $XPB^{+/-}$ cells displayed the effects of oxidative stress later than the other two cell types. It is possible that this is a result of a heterozygote effect granting increased tolerance to oxidative stress without overly deleterious effects. The above mentioned partially redundant role of XPB in apoptotic signaling may offer an explanation as one functional copy of the gene is able to compensate along with the other partially redundant factors for the dysfunctional copies. $XPB^{-/-}$ cells would more handicapped in this manner and perhaps less adept at compensating under stress.

As well as these morphological changes and marker expression, we observed a heightened telomere attrition rate under oxidative stress, especially when combined with lack of one of both copies of functional XPB. Telomeres cap chromosomal ends and are important for chromosome integrity and segregation at mitosis (Hande et al., 1999a; Slijepcevic et al., 1997; Blasco et al., 1997). They have also been long regarded as a determinant in cellular replication, aging and lifespan (Rodier et al., 2005; Shay and Wright, 2001; Gilley et al., 2005; Klapper et al., 2001; Levy et al., 1992; Rodier et al., 2005). Telomeres have been shown to preferentially accumulate single stranded regions induced by oxidative stress (Petersen et al., 1998). Various factors, such as the telomere repeating binding factors TRF1 and TRF2 and telomerase, modulate telomeres dynamics and integrity (Rodier et al., 2005). It also has been found that DNA repair factors such as ATM, WRN and BLM function in telomere maintenance and repair of damage sustained at telomeres (Bai and Murnane, 2003; Crabbe et al., 2004; Crabbe et al., 2007; Du et al.,

2004; Eller et al., 2006; Lillard-Wetherell et al., 2005; Opresko et al., 2002; Opresko et al., 2005; Schawalder et al., 2003; Stavropoulos et al., 2002; Tchirkov and Lansdorp, 2003; Hande et al., 2001). The latter two proteins belong to the helicase domain containing family of proteins of which XPB is also a member. This family of proteins has been implicated in genomic stability, telomere maintenance and aging (Du et al., 2004; Nakura et al., 2000; van Brabant et al., 2000). As such, though the presence of increased telomere attrition in $XPB^{-/-}$ cells is not an unexpected result it is a novel observation. Further support comes from studies that show XPF, one of the partner proteins of XPB in the NER pathway is involved in telomere dynamics in mice (Munoz et al., 2005). Our findings corroborate evidence that helicase domain containing proteins are major players in telomere function and modulation. Moreover, these results further suggest oxidative stress as a contributing factor for the premature aging symptoms presented by XP-B patients, particularly for tissues away from the body surface.

Taking note of the functional outcomes of exposure to H_2O_2, we were interested in understanding the mechanisms behind these phenomena. To this end, Western blotting was performed for XPB as well as a series of cell cycle proteins. We selected a dose of 40 μM as this was the concentration at which differences between Normal and $XPB^{-/-}$ cells were first observed in the majority of assays. A 48 hour time point was also included to allow for the 48 hour intervals used in the cellular kinetics assays.

In Normal cells XPB displays upregulation following exposure to H_2O_2, consistent with previous assays and our hypothesis of a role for XPB in oxidative stress response. Interestingly, XPB upregulation occurs at divergent time points in Normal cells (24 hours) and $XPB^{+/-}$ cells (2 hours). This might be explained by the lower levels of

XPB in $XPB^{+/-}$ cells. These cells would thus require an earlier increase in XPB levels following oxidative stress whereas Normal cells have a sufficient baseline reservoir allowing for later upregulation.

p53 is a cell cycle checkpoint protein regarded as the guardian of the genome. It undergoes changes in expression level as well as post-translational modifications such as phosphorylation following genotoxic stress. Phosphorylation at the serine 15 residue is a marker of DNA damage. We observed both p53 upregulation and phosphorylation in all three cell types with exposure to H_2O_2. p53 expression and phosphorylation patterns showed a difference in Normal and $XPB^{-/-}$ cells. In Normal cells, increased phosphorylation was observed first at 2 hours with upregulation following at 24 hours, with reversion of both to baseline levels at 48 hours. $XPB^{-/-}$ cells displayed upregulation at 2 hours and increased phosphorylation at 48 hours. $XPB^{+/-}$ cells displayed intermediate patterns. XPB was reported to be able to bind to p53 (Wang et al., 1995; Leveillard et al., 1996) and have a partially redundant role in p53-mediated apoptotic signalling (Spillare et al., 2006; Bernstein et al., 2002). This might account for the conundrum of increased genotoxicity with decreased cytotoxicity. Lack of functional XPB in $XPB^{-/-}$ cells might compromise the ability of these cells to properly phosphorylate p53 and trigger DNA damage and possibly apoptotic signalling cascades. This is in agreement with the results of the Crystal Violet assay showing higher viability in $XPB^{-/-}$ cells following H_2O_2 treatment. The presence of increased p53 phosphorylation in $XPB^{-/-}$ cells at 48 hours also corroborates the results of the Comet assay which indicate compromised recovery and persistence of DNA damage after resolution in Normal cells. The earlier increased

expression of p53 in these cells might be an attempt to overcome their inability to phosphorylate p53.

Numerous reports have shown that a number of DNA repair proteins (Hande, 2004) have telomere function and/or interaction with telomeres or telomere associated proteins. These include ATM (Tchirkov and Lansdorp, 2003) as well as WRN and BLM (Bai and Murnane, 2003; Crabbe et al., 2004; Crabbe et al., 2007; Du et al., 2004; Eller et al., 2006; Klapper et al., 2001; Lee et al., 2005; Lillard-Wetherell et al., 2005; Multani and Chang, 2007; Opresko et al., 2002; Opresko et al., 2005; Orren, 2006; Schawalder et al., 2003; Stavropoulos et al., 2002). The latter two proteins are helicases like XPB and are involved in repair of oxidative DNA lesions via the base excision repair (BER) pathway (Hoeijmakers, 2001). XPB, WRN and BLM have all been shown to bind to p53 and WRN and BLM are reported to physically interact with TRF2. These findings together with the accelerated telomere attrition we observed in our cellular kinetics study motivated our immunofluorescence experiments. We were however unable to detect any co-localization of XPB with either TRF2 or with telomeres under our experimental conditions.

XPB was found to physically interact with p53 in overexpression studies. Given the differential expression and upregulation patterns in our experiments we sought to investigate if native XPB interacts with p53 and if so, whether this interaction was affected by oxidative stress. The fibroblasts used in the earlier assays were unsuitable for such analysis as they exhibited replicative senescence and had a slow doubling time resulting in insufficient numbers of cells. HeLa cells which were used in the immunofluorescence assays were likewise incompatible as they do not have the large

amounts of p53 required for an experiment involving p53 interactions. We thus utilized lymphoblastoid cells for co-immunoprecipitation of XPB and p53 as these cells were able to provide the large quantities of protein required for the assay. The total cell lysates for co-immunoprecipitation showed similar patterns to our earlier Western blots, indicating similar in both fibroblasts and lymphoblastoid cells. Using XPB as bait protein and p53 as prey and vice versa, we did not detect any physical interaction by co-immunoprecipitation.

It is possible that interactions between XPB and TRF2, telomeres and p53 occur transiently and/or are weak interactions which are difficult to detect under our treatments and with endogenous proteins. Overexpression of proteins using tags such as GST as well as increasing the concentration of H_2O_2 could yield positive interactions. It should be also noted that lack of physical interactions does not translate to absence of functional interaction or pathway cross-talk. Particularly, the NER pathway features not only spatial but temporal coordination of its factors (Hoeijmakers, 2001). Each member of the pathway is recruited to the same lesion at different points following genotoxic insult and do not necessarily interact physically. Instead, some proteins verify the presence of damage and modify and stabilize repair intermediates for the entry of subsequent factors. This makes it difficult to capture physical interactions or colocalizations at a single point in time. Live cell imaging of XPB distribution patterns with respect to those TRF2, telomeres and p53 following oxidative stress might therefore give greater perspectives on the molecular clockwork involving XPB and oxidative stress. Furthermore, it has been demonstrated that in the case of another NER protein, CSB, lack of functional protein resulted in misregulation in the expression of numerous genes related to transcription,

translation, signal transduction and cell cycle progression (Kyng et al., 2003). Similar to XPB, CSB is also a helicase and is believed to be a transcription factor (ref Lee et al, 2001). It is thus possible that dysfunction in XPB might result in similar consequences following oxidative stress. Microarray and superarray analysis of gene expression levels following H_2O_2 induced oxidative stress in both Normal and XPB cells would give much insight into this aspect.

Our results thus support previous findings on XPB and extend them towards oxidative stress resistance. As discussed previously, failure in the ability of cells to properly detect and respond to DNA damage by executing repair and/or apoptosis is a potentially hazardous situation with outcomes including mutagenesis and oncogenesis.

CHAPTER 6

LIMITATIONS OF STUDY AND FUTURE WORKS

LIMITATIONS OF CURRENT STUDY AND FUTURE WORKS

It is important to note that our study was conducted under *in vitro* conditions which may be not completely mirrored *in vivo*. For instance, oxidative stress acts primarily as a life long condition while the longest assay in this study lasted 30 days. The levels of stress induced in our treatments are also unlikely to be the same as those present in physiological conditions. In addition, H_2O_2 is the one of the most abundant endogenously produced reactive oxygen species, it is not the only one which contributes to physiological oxidative stress. Further insight into the role of XPB will have to address these issues. Future experiments would thus involve culturing cells for a longer period of time under oxidative stress. A contrast study can also be included by growing cells under conditions in which oxidative stress is reduced, such as in the presence of anti-oxidants or in a low oxygen incubator. Other inducers of oxidative stress such as arsenite and nitric oxide may also be utilized to investigate if the observed findings are common to all forms of oxidative stress or particular to H_2O_2.

Although we did not detect any physical interactions between XPB and TRF2 or p53, it is not evidence of any absence of interaction. It is possible that such interactions may be cell cycle stage dependant. Thus the immunofluorescence and co-immunoprecipitation may be conducted at different stages of the cell cycle after arrest and synchronisation of cells with agents such as hydroxyurea. The results of cellular kinetics and telomere dynamics experiments are another area which may be expanded on. Chromatin Immunoprecipitation (ChIP) targeting XPB and telomeric DNA sequences can be carried out to elucidate if such interactions exist and the conditions in which they occur.

Finally, the lack of physical interactions does not rule out functional interactions. To pursue this line of inquiry, siRNA may be used to silence TRF2 and p53 in Normal as well as XPB deficient cells in order to study the effect of multiple deficiencies on genome stability.

CHAPTER 7

CONCLUSION

CONCLUSION

In summary, our study has shown that the dysfunction in XPB sensitizes cells to the genotoxic effects of oxidative stress while reducing the cytotoxic effects. Such a phenomenon can result in genome instability which can predispose cancer and accelerated telomere attrition which may influence aging. This is congruent with XP patients being extremely sensitive to UV-induced skin lesions and cancers. It is however hard for UV-induced DNA damage to explain the full range of XP symptoms. Our findings thus implicate oxidative stress as a possible major contributor to such manifestations, particularly at tissues away from the body surface and hence protected from UV exposure and complements present knowledge regarding XP. This is not surprising given that oxidative stress via ROS generation is downstream to a various other genotoxic agents including UV-irradiation (Finkel and Holbrook, 2000). It has been shown that polymorphisms in the XPB gene can rise to diseases of varying severities and phenotypes (Oh et al., 2006). Additionally, the inclusion of heterozygous cells in our study hint as well at a possible copy number dependence. In line with our hypothesis we have also shown that XPB is differentially regulated and distributed following oxidative insult and is a player in mediating the functions of crucial cell cycle proteins such as p53. Our results also indicate a role for XPB in the resolution of oxidative stress induced DNA lesions and in telomere dynamics. A recent report suggests that the helicase activity of XPB in NER repair of UV induced DNA lesions is dispensable while its ATPase activity is essential (Coin et al., 2007). Whether this is also true of repair of oxidative lesions and telomere maintenance is, and whether these activities are performed exclusively by XPB

or in concert with other factors including the rest of the NER and telomere binding proteins is the subject of further research.

CHAPTER 8

APPENDIX

APPENDIX

Supplemented Minimal Essential Medium for adherent cell culture:

Minimal Essential Medium
15% Fetal Bovine Serum
100 U/ml penicillin/streptomycin
1% Vitamins
2% Essential Amino Acids
1% Non-essential Amino Acids

Supplemented Roswell Park Memorial Institute 1640 Medium for lymphoblastoid culture:

Roswell Park Memorial Institute 1640 Medium
15% Fetal Bovine Serum
1% L-Glutamine

Crystal Violet Solution:

0.25% NaCl
0.75% Crystal Violet
1.75% Formaldehyde
50% Ethanol

Comet Lysis Solution:

2.5 M NaCl
0.1 M EDTA pH 8.0
10 mM Tris base
1% Triton X-100

Comet Electrophoresis Buffer:

0.3 M NaOH buffered at pH 13.0 -13.8 with 0.5 M EDTA

Carnoy's Fixative:

3:1 Methanol : Acetic Acid

Western Blot Denaturing Lysis Buffer:

10 mM Tris-HCl pH 7.4

1% Sodium Dodecyl Sulfate

1 mM Sodium Orthovanadate

PNA FISH Hybridization Mix:

70% Deionized Formamide

0.25% Blocking Reagent in Maleic Acid Buffer

10 mM Tris

5% $MgCl_2$ Buffer

0.5 µg/ml PNA-Tel probe

Maleic Acid Buffer:

0.1M Maleic Acid

0.15M NaCl

pH adjusted to 7.5 with NaOH

2.5% Blocking Reagent in Maleic Acid Buffer:

0.25 g Blocking Reagent (Boehringer, Germany) in Maleic Acid Buffer

$MgCl_2$ Buffer:

25 mM $MgCl_2$

9 mM Citric Acid

82 mM Na_2PO_4

PNA FISH Wash Solution 1:

70 % Formamide

0.1% Bovine Serum Albumin

0.01 M Tris-HCl pH 7.4

PNA FISH Wash Solution 2:

0.1 M Tris

0.15 M NaCl

0.07% Tween-20

Co-Immunoprecipitation Non Denaturing Lysis Buffer:

50 mM Tris-HCl pH 8.0

5 mM EDTA pH 8.0

150 nM NaCl

0.5% Triton X-100

1 mM Phenylmethanesulphonyl Fluoride

1 mM Sodium Orthovanadate

½ tablet Roche Complete Mini per 5 ml of lysis buffer

Co-Immunoprecipitation Wash Buffer:

50 mM Tris-HCl ph 7.4

150 nM NaCl

5 mM EDTA pH 8.0

0.1% Triton X-100

CHAPTER 9

REFERENCES

REFERENCE LIST

Akoulitchev,S., Makela,T.P., Weinberg,R.A., and Reinberg,D. (1995). Requirement for TFIIH kinase activity in transcription by RNA polymerase II. Nature *377*, 557-560.

Bai,Y. and Murnane,J.P. (2003). Telomere instability in a human tumor cell line expressing a dominant-negative WRN protein. Hum. Genet. *113*, 337-347.

Barzilai,A. and Yamamoto,K. (2004). DNA damage responses to oxidative stress. DNA Repair (Amst) *3*, 1109-1115.

Bernstein,C., Bernstein,H., Payne,C.M., and Garewal,H. (2002). DNA repair/pro-apoptotic dual-role proteins in five major DNA repair pathways: fail-safe protection against carcinogenesis. Mutat. Res. *511*, 145-178.

Blasco,M.A., Lee,H.W., Hande,M.P., Samper,E., Lansdorp,P.M., DePinho,R.A., and Greider,C.W. (1997). Telomere shortening and tumor formation by mouse cells lacking telomerase RNA. Cell *91*, 25-34.

Bradshaw,P.S., Stavropoulos,D.J., and Meyn,M.S. (2005). Human telomeric protein TRF2 associates with genomic double-strand breaks as an early response to DNA damage. Nat. Genet. *37*, 193-197.

Brooks,P.J., Wise,D.S., Berry,D.A., Kosmoski,J.V., Smerdon,M.J., Somers,R.L., Mackie,H., Spoonde,A.Y., Ackerman,E.J., Coleman,K., Tarone,R.E., and Robbins,J.H. (2000). The oxidative DNA lesion 8,5'-(S)-cyclo-2'-deoxyadenosine is repaired by the nucleotide excision repair pathway and blocks gene expression in mammalian cells. J. Biol. Chem. *275*, 22355-22362.

Chen,Q. and Ames,B.N. (1994). Senescence-like growth arrest induced by hydrogen peroxide in human diploid fibroblast F65 cells. Proc. Natl. Acad. Sci. U. S. A *91*, 4130-4134.

Coin,F., Auriol,J., Tapias,A., Clivio,P., Vermeulen,W., and Egly,J.M. (2004). Phosphorylation of XPB helicase regulates TFIIH nucleotide excision repair activity. EMBO J. *23*, 4835-4846.

Coin,F., Oksenych,V., and Egly,J.M. (2007). Distinct roles for the XPB/p52 and XPD/p44 subcomplexes of TFIIH in damaged DNA opening during nucleotide excision repair. Mol. Cell *26*, 245-256.

Collins,A.R. (2004). The comet assay for DNA damage and repair: principles, applications, and limitations. Mol. Biotechnol. *26*, 249-261.

Crabbe,L., Jauch,A., Naeger,C.M., Holtgreve-Grez,H., and Karlseder,J. (2007). Telomere dysfunction as a cause of genomic instability in Werner syndrome. Proc. Natl. Acad. Sci. U. S. A *104*, 2205-2210.

Crabbe,L., Verdun,R.E., Haggblom,C.I., and Karlseder,J. (2004). Defective telomere lagging strand synthesis in cells lacking WRN helicase activity. Science *306*, 1951-1953.

d'Adda,d.F.F., Hande,M.P., Tong,W.M., Lansdorp,P.M., Wang,Z.Q., and Jackson,S.P. (1999). Functions of poly(ADP-ribose) polymerase in controlling telomere length and chromosomal stability. Nat. Genet. *23*, 76-80.

d'Adda,d.F.F., Hande,M.P., Tong,W.M., Roth,D., Lansdorp,P.M., Wang,Z.Q., and Jackson,S.P. (2001). Effects of DNA nonhomologous end-joining factors on telomere length and chromosomal stability in mammalian cells. Curr. Biol. *11*, 1192-1196.

de Boer,J., Andressoo,J.O., de,W.J., Huijmans,J., Beems,R.B., van,S.H., Weeda,G., van der Horst,G.T., van,L.W., Themmen,A.P., Meradji,M., and Hoeijmakers,J.H. (2002). Premature aging in mice deficient in DNA repair and transcription. Science *296*, 1276-1279.

Dizdaroglu,M. (1992). Oxidative damage to DNA in mammalian chromatin. Mutat. Res. *275*, 331-342.

Du,X., Shen,J., Kugan,N., Furth,E.E., Lombard,D.B., Cheung,C., Pak,S., Luo,G., Pignolo,R.J., DePinho,R.A., Guarente,L., and Johnson,F.B. (2004). Telomere shortening exposes functions for the mouse Werner and Bloom syndrome genes. Mol. Cell Biol. *24*, 8437-8446.

Duan,J., Duan,J., Zhang,Z., and Tong,T. (2005). Irreversible cellular senescence induced by prolonged exposure to H2O2 involves DNA-damage-and-repair genes and telomere shortening. Int. J. Biochem. Cell Biol. *37*, 1407-1420.

Eller,M.S., Liao,X., Liu,S., Hanna,K., Backvall,H., Opresko,P.L., Bohr,V.A., and Gilchrest,B.A. (2006). A role for WRN in telomere-based DNA damage responses. Proc. Natl. Acad. Sci. U. S. A *103*, 15073-15078.

Fenech,M. (2000). The in vitro micronucleus technique. Mutat. Res. *455*, 81-95.

Finkel,T. and Holbrook,N.J. (2000). Oxidants, oxidative stress and the biology of ageing. Nature *408*, 239-247.

Gilley,D., Tanaka,H., Hande,M.P., Kurimasa,A., Li,G.C., Oshimura,M., and Chen,D.J. (2001). DNA-PKcs is critical for telomere capping. Proc. Natl. Acad. Sci. U. S. A *98*, 15084-15088.

Gilley,D., Tanaka,H., and Herbert,B.S. (2005). Telomere dysfunction in aging and cancer. Int. J. Biochem. Cell Biol. *37*, 1000-1013.

Greenwood,S.K., Hill,R.B., Sun,J.T., Armstrong,M.J., Johnson,T.E., Gara,J.P., and Galloway,S.M. (2004). Population doubling: a simple and more accurate estimation of cell growth suppression in the in vitro assay for chromosomal aberrations that reduces irrelevant positive results. Environ. Mol. Mutagen. *43*, 36-44.

Halliwell,B. and Gutteridge,J.M. (1992). Biologically relevant metal ion-dependent hydroxyl radical generation. An update. FEBS Lett. *307*, 108-112.

Hande,M.P. (2004). DNA repair factors and telomere-chromosome integrity in mammalian cells. Cytogenet. Genome Res. *104*, 116-122.

Hande,M.P., Balajee,A.S., Tchirkov,A., Wynshaw-Boris,A., and Lansdorp,P.M. (2001). Extra-chromosomal telomeric DNA in cells from Atm(-/-) mice and patients with ataxia-telangiectasia. Hum. Mol. Genet. *10*, 519-528.

Hande,M.P., Boei,J.J., and Natarajan,A.T. (1996). Induction and persistence of cytogenetic damage in mouse splenocytes following whole-body X-irradiation analysed by fluorescence in situ hybridization. II. Micronuclei. Int. J. Radiat. Biol. *70*, 375-383.

Hande,M.P., Samper,E., Lansdorp,P., and Blasco,M.A. (1999a). Telomere length dynamics and chromosomal instability in cells derived from telomerase null mice. J. Cell Biol. *144*, 589-601.

Hande,P., Slijepcevic,P., Silver,A., Bouffler,S., van,B.P., Bryant,P., and Lansdorp,P. (1999b). Elongated telomeres in scid mice. Genomics *56*, 221-223.

Harman,D. (1956). Aging: a theory based on free radical and radiation chemistry. J. Gerontol. *11*, 298-300.

Hayflick,L. and Moorhead,P.S. (1961). The serial cultivation of human diploid cell strains. Exp. Cell Res. *25*, 585-621.

Hoeijmakers,J.H. (2001). Genome maintenance mechanisms for preventing cancer. Nature *411*, 366-374.

Hsu,H.L., Gilley,D., Galande,S.A., Hande,M.P., Allen,B., Kim,S.H., Li,G.C., Campisi,J., Kohwi-Shigematsu,T., and Chen,D.J. (2000). Ku acts in a unique way at the mammalian telomere to prevent end joining. Genes Dev. *14*, 2807-2812.

Hu,G.M., Liu,L.M., Zhang,J.X., Hu,X.D., Duan,H.J., Deng,H., He,M., Luo,Z.J., Liu,J.M., and Luo,J. (2006). The role of XPB in cell apoptosis and viability and its relationship with p53, p21(waf1/cip1) and c-myc in hepatoma cells. Dig. Liver Dis. *38*, 755-761.

Iliakis,G., Wang,Y., Guan,J., and Wang,H. (2003). DNA damage checkpoint control in cells exposed to ionizing radiation. Oncogene *22*, 5834-5847.

Imlay,J.A., Chin,S.M., and Linn,S. (1988). Toxic DNA damage by hydrogen peroxide through the Fenton reaction in vivo and in vitro. Science *240*, 640-642.

Kashino,G., Kodama,S., Nakayama,Y., Suzuki,K., Fukase,K., Goto,M., and Watanabe,M. (2003). Relief of oxidative stress by ascorbic acid delays cellular senescence of normal human and Werner syndrome fibroblast cells. Free Radic. Biol. Med. *35*, 438-443.

Klapper,W., Parwaresch,R., and Krupp,G. (2001). Telomere biology in human aging and aging syndromes. Mech. Ageing Dev. *122*, 695-712.

Kraemer,K.H., Patronas,N.J., Schiffmann,R., Brooks,B.P., Tamura,D., and DiGiovanna,J.J. (2007). Xeroderma pigmentosum, trichothiodystrophy and Cockayne syndrome: a complex genotype-phenotype relationship. Neuroscience *145*, 1388-1396.

Kumazaki,T., Robetorye,R.S., Robetorye,S.C., and Smith,J.R. (1991). Fibronectin expression increases during in vitro cellular senescence: correlation with increased cell area. Exp. Cell Res. *195*, 13-19.

Kuraoka,I., Bender,C., Romieu,A., Cadet,J., Wood,R.D., and Lindahl,T. (2000). Removal of oxygen free-radical-induced 5',8-purine cyclodeoxynucleosides from DNA by the nucleotide excision-repair pathway in human cells. Proc. Natl. Acad. Sci. U. S. A *97*, 3832-3837.

Kyng,K.J., May,A., Brosh,R.M., Jr., Cheng,W.H., Chen,C., Becker,K.G., and Bohr,V.A. (2003). The transcriptional response after oxidative stress is defective in Cockayne syndrome group B cells. Oncogene *22*, 1135-1149.

Lee,J.W., Harrigan,J., Opresko,P.L., and Bohr,V.A. (2005). Pathways and functions of the Werner syndrome protein. Mech. Ageing Dev. *126*, 79-86.

Lehmann,A.R. (1995). Nucleotide excision repair and the link with transcription. Trends Biochem. Sci. *20*, 402-405.

Leveillard,T., Andera,L., Bissonnette,N., Schaeffer,L., Bracco,L., Egly,J.M., and Wasylyk,B. (1996). Functional interactions between p53 and the TFIIH complex are affected by tumour-associated mutations. EMBO J. *15*, 1615-1624.

Levy,M.Z., Allsopp,R.C., Futcher,A.B., Greider,C.W., and Harley,C.B. (1992). Telomere end-replication problem and cell aging. J. Mol. Biol. *225*, 951-960.

Lillard-Wetherell,K., Combs,K.A., and Groden,J. (2005). BLM helicase complements disrupted type II telomere lengthening in telomerase-negative sgs1 yeast. Cancer Res. *65*, 5520-5522.

Lindenbaum,Y., Dickson,D., Rosenbaum,P., Kraemer,K., Robbins,I., and Rapin,I. (2001). Xeroderma pigmentosum/cockayne syndrome complex: first

neuropathological study and review of eight other cases. Eur. J. Paediatr. Neurol. *5*, 225-242.

Low,G.K., Fok,E.D., Ting,A.P., and Hande,M.P. (2008). Oxidative damage induced genotoxic effects in human fibroblasts from Xeroderma Pigmentosum group A patients. Int. J. Biochem. Cell Biol.

Marini,F., Nardo,T., Giannattasio,M., Minuzzo,M., Stefanini,M., Plevani,P., and Falconi,M.M. (2006). DNA nucleotide excision repair-dependent signaling to checkpoint activation. Proc. Natl. Acad. Sci. U. S. A *103*, 17325-17330.

McKinnon,P.J. (2004). ATM and ataxia telangiectasia. EMBO Rep. *5*, 772-776.

McPherson,J.P., Hande,M.P., Poonepalli,A., Lemmers,B., Zablocki,E., Migon,E., Shehabeldin,A., Porras,A., Karaskova,J., Vukovic,B., Squire,J., and Hakem,R. (2006). A role for Brca1 in chromosome end maintenance. Hum. Mol. Genet. *15*, 831-838.

mor-Gueret,M. (2006). Bloom syndrome, genomic instability and cancer: the SOS-like hypothesis. Cancer Lett. *236*, 1-12.

Multani,A.S. and Chang,S. (2007). WRN at telomeres: implications for aging and cancer. J. Cell Sci. *120*, 713-721.

Munoz,P., Blanco,R., Flores,J.M., and Blasco,M.A. (2005). XPF nuclease-dependent telomere loss and increased DNA damage in mice overexpressing TRF2 result in premature aging and cancer. Nat. Genet. *37*, 1063-1071.

Nakura,J., Ye,L., Morishima,A., Kohara,K., and Miki,T. (2000). Helicases and aging. Cell Mol. Life Sci. *57*, 716-730.

Norgauer,J., Idzko,M., Panther,E., Hellstern,O., and Herouy,Y. (2003). Xeroderma pigmentosum. Eur. J. Dermatol. *13*, 4-9.

Oh,K.S., Imoto,K., Boyle,J., Khan,S.G., and Kraemer,K.H. (2007). Influence of XPB helicase on recruitment and redistribution of nucleotide excision repair proteins at sites of UV-induced DNA damage. DNA Repair (Amst).

Oh,K.S., Khan,S.G., Jaspers,N.G., Raams,A., Ueda,T., Lehmann,A., Friedmann,P.S., Emmert,S., Gratchev,A., Lachlan,K., Lucassan,A., Baker,C.C., and Kraemer,K.H. (2006). Phenotypic heterogeneity in the XPB DNA helicase gene (ERCC3): xeroderma pigmentosum without and with Cockayne syndrome. Hum. Mutat. *27*, 1092-1103.

Opresko,P.L., Mason,P.A., Podell,E.R., Lei,M., Hickson,I.D., Cech,T.R., and Bohr,V.A. (2005). POT1 stimulates RecQ helicases WRN and BLM to unwind telomeric DNA substrates. J. Biol. Chem. *280*, 32069-32080.

Opresko,P.L., von Kobbe,C., Laine,J.P., Harrigan,J., Hickson,I.D., and Bohr,V.A. (2002). Telomere-binding protein TRF2 binds to and stimulates the Werner and Bloom syndrome helicases. J. Biol. Chem. *277*, 41110-41119.

Orren,D.K. (2006). Werner syndrome: molecular insights into the relationships between defective DNA metabolism, genomic instability, cancer and aging. Front Biosci. *11*, 2657-2671.

Petersen,S., Saretzki,G., and von Zglinicki,T. (1998). Preferential accumulation of single-stranded regions in telomeres of human fibroblasts. Exp. Cell Res. *239*, 152-160.

Rapin,I., Lindenbaum,Y., Dickson,D.W., Kraemer,K.H., and Robbins,J.H. (2000). Cockayne syndrome and xeroderma pigmentosum. Neurology *55*, 1442-1449.

Rodier,F., Kim,S.H., Nijjar,T., Yaswen,P., and Campisi,J. (2005). Cancer and aging: the importance of telomeres in genome maintenance. Int. J. Biochem. Cell Biol. *37*, 977-990.

Rybanska,I. and Pirsel,M. (2003). Involvement of the nucleotide excision repair proteins in the removal of oxidative DNA base damage in mammalian cells. Neoplasma *50*, 389-395.

Sancar,A. (1996). DNA excision repair. Annu. Rev. Biochem. *65*, 43-81.

Satoh,M.S., Jones,C.J., Wood,R.D., and Lindahl,T. (1993). DNA excision-repair defect of xeroderma pigmentosum prevents removal of a class of oxygen free radical-induced base lesions. Proc. Natl. Acad. Sci. U. S. A *90*, 6335-6339.

Schawalder,J., Paric,E., and Neff,N.F. (2003). Telomere and ribosomal DNA repeats are chromosomal targets of the bloom syndrome DNA helicase. BMC. Cell Biol. *4*, 15.

Serra,V., von Zglinicki,T., Lorenz,M., and Saretzki,G. (2003). Extracellular superoxide dismutase is a major antioxidant in human fibroblasts and slows telomere shortening. J. Biol. Chem. *278*, 6824-6830.

Shackelford,R.E., Kaufmann,W.K., and Paules,R.S. (2000). Oxidative stress and cell cycle checkpoint function. Free Radic. Biol. Med. *28*, 1387-1404.

Shay,J.W. and Wright,W.E. (2001). Telomeres and telomerase: implications for cancer and aging. Radiat. Res. *155*, 188-193.

Slijepcevic,P., Hande,M.P., Bouffler,S.D., Lansdorp,P., and Bryant,P.E. (1997). Telomere length, chromatin structure and chromosome fusigenic potential. Chromosoma *106*, 413-421.

Spillare,E.A., Wang,X.W., von Kobbe,C., Bohr,V.A., Hickson,I.D., and Harris,C.C. (2006). Redundancy of DNA helicases in p53-mediated apoptosis. Oncogene *25*, 2119-2123.

Stansel,R.M., de,L.T., and Griffith,J.D. (2001). T-loop assembly in vitro involves binding of TRF2 near the 3' telomeric overhang. EMBO J. *20*, 5532-5540.

Stavropoulos,D.J., Bradshaw,P.S., Li,X., Pasic,I., Truong,K., Ikura,M., Ungrin,M., and Meyn,M.S. (2002). The Bloom syndrome helicase BLM interacts with TRF2 in ALT cells and promotes telomeric DNA synthesis. Hum. Mol. Genet. *11*, 3135-3144.

Sugasawa,K. (2008). Xeroderma pigmentosum genes: functions inside and outside DNA repair. Carcinogenesis *29*, 455-465.

Tchirkov,A. and Lansdorp,P.M. (2003). Role of oxidative stress in telomere shortening in cultured fibroblasts from normal individuals and patients with ataxia-telangiectasia. Hum. Mol. Genet. *12*, 227-232.

van Brabant,A.J., Stan,R., and Ellis,N.A. (2000). DNA helicases, genomic instability, and human genetic disease. Annu. Rev. Genomics Hum. Genet. *1*, 409-459.

van Steeg,H. and Kraemer,K.H. (1999). Xeroderma pigmentosum and the role of UV-induced DNA damage in skin cancer. Mol. Med. Today *5*, 86-94.

von Zglinicki,T. (2002). Oxidative stress shortens telomeres. Trends Biochem. Sci. *27*, 339-344.

Wakasugi,M. and Sancar,A. (1998). Assembly, subunit composition, and footprint of human DNA repair excision nuclease. Proc. Natl. Acad. Sci. U. S. A *95*, 6669-6674.

Wang,X.W., Yeh,H., Schaeffer,L., Roy,R., Moncollin,V., Egly,J.M., Wang,Z., Freidberg,E.C., Evans,M.K., Taffe,B.G., and . (1995). p53 modulation of TFIIH-associated nucleotide excision repair activity. Nat. Genet. *10*, 188-195.

Wood,R.D. (1997). Nucleotide excision repair in mammalian cells. J. Biol. Chem. *272*, 23465-23468.

LIST OF CONFERENCES ATTENDED

1. **Ting APL**, Low GKM, Hande MP. *Role of XPB in genome maintenance under oxidative stress.* Genetic Toxicology. Gordon Research Conferences, Genetic Toxicology Conference, Oxford, UK. July 29th to August 3rd, 2007.

2. **Ting APL**, Low GKM, Hande MP. *Oxidative-stress induced genome instability in cells derived from Xeroderma Pigmentosum B patients.* National Healthcare Group, Annual Scientific Congress, Singapore, November 10th to 11th, 2007.

3. Low GKM, **Ting APL**, Hande MP. *Role of Nucleotide Excision Repair factors in genome maintenance under oxidative-stress.* Gordon Research Conferences, DNA Damage, Mutation and Cancer Conference, Oxford, UK. March 9th to 14th 2007

4. Low GKM, **Ting APL**, Gopalakrishnan K, Hande MP. *Role of Nucleotide Repair factors in Genome Stability under Oxidative Stress.* Gordon Research Conferences, Mutagenesis Conference, Oxford, UK. July 20th to 26th 2008.

LIST OF PUBLICATIONS

1. Low GKM, Fok EDZ, **Ting APL**, Hande MP. 2008. *Oxidative damage induced genotoxic effects in human fibroblasts from Xeroderma Pigmentosum A patients*. **International Journal of Biochemistry and Cell Biology**

2. **Ting APL**, Low GKM, Hande MP. 2008. *Telomere attrition and genomic instability in Xeroderma Pigmentosum type-B deficient fibroblasts under oxidative stress*. **(Submitted and under review)**

LIST OF AWARDS

1. Best Oral Presentation Award (Basic Sciences) for *Oxidative-stress induced genome instability in cells derived from Xeroderma Pigmentosum B patients* at National Healthcare Group Annual Scientific Congress, Singapore, November 10th to 11th, 2007